



## Invited review article

# Precipitation and drought trends (1952–2021) in a key hydrological recharge area of the eastern Iberian Peninsula

Juan Javier Miró<sup>a</sup>, María José Estrela<sup>a</sup>, David Corell<sup>a,\*</sup>, Igor Gómez<sup>b,c</sup>, María Yolanda Luna<sup>d</sup>

<sup>a</sup> Department of Geography, Faculty of Geography and History, University of Valencia, Av. Blasco Ibáñez 28, Valencia 46010, Spain

<sup>b</sup> Department of Applied Physics, Faculty of Physics, University of Alicante, Crta. San Vicente del Raspeig, s/n, 03080 Alicante, Spain

<sup>c</sup> Multidisciplinary Institute for Environmental Studies (MIES) “Ramón Margalef”, University of Alicante, Crta. San Vicente del Raspeig, s/n, Alicante 03080, Spain

<sup>d</sup> State Meteorological Agency (AEMET), Madrid, Spain

## ARTICLE INFO

## Keywords:

Annual and seasonal trends

Dry spell

Climate change

Precipitation

SPEI

Drought

## ABSTRACT

The objective of the study is to quantify the effect of climate change on the climatic risks associated with droughts and diminished water resources in the eastern Iberian Peninsula. For this purpose, this work analyses the 70-year historical series (1952–2021) of daily rainfall data from 353 meteorological stations. They are located in a key recharge area of the hydrological system, the *Sierra de Albarracín*, where three important rivers originate, namely the Tagus, the Júcar and the Turia, as do several tributaries of the Guadiana and Ebro rivers. It analyses trends in: annual and seasonal rainfall volumes with specific studies about their intensity according to certain percentiles; the number of rainy days, dry spell duration (< 1 mm/day) and drought evolution with the Standardized Precipitation Evaporation Index. The most relevant results are: (1) the second 35 years of the study period (1987–2021) were notably drier than the first part (1952–1986), with smaller volumes and fewer days with recorded precipitation; (2) summer and winter were most affected by pluviometric decrease, with losses of >50% of rainfall volume at some stations; (3) moderate rainfall significantly reduced between the 50th and 95th percentiles, which were more important in the system's water recharge; (4) the stations with a negative precipitation trend predominated; (5) the medium- and long-term analyses (12 and 36 months) highlighted the drought situation in which the headwaters of the analyzed basins are immersed. The trend indicates that the situation will become critical.

## 1. Introduction

Climate change is a major threat that humanity faces in the 21st century. It puts the environment at risk and implicates not only society, economy and growth, but also development models. Numerous studies predict that such changes will lead to more extreme heat waves, and also to severer and more persistent droughts. Water is an indispensable resource for human life. Any change in precipitation patterns can disrupt its availability and, thus, have profound effects on society and nature (Randall et al., 2007). In this context, it should be highlighted that since 1950, changes in extreme weather and climate events have been observed, such as increases in the frequency and intensity of heavy precipitation and, therefore, of floods (Intergovernmental Panel on Climate Change (IPCC), 2022; Giorgi, 2006). With this critical change aspect, the Mediterranean region is a clear example of this situation. In fact, the Mediterranean basin has been defined as a hot spot for global

warming (Giorgi, 2006; Lionello et al., 2012; Lionello and Scarascia, 2018), where forecasts indicate a generalized rise in temperature and decreased precipitation that will mean serious water supply problems for the region (Christensen et al., 2007; Cos et al., 2022; Gualdi et al., 2013; Ulbrich et al., 2013).

There is no doubt that the hydrological cycle in the Mediterranean basin will be profoundly affected by climate change. Different studies predict that less rain will fall in the basin due to not only the increased divergence of water vapor in subtropical areas, which will move toward the poles (Held and Soden, 2006), but also the contraction of the circumpolar vortex (Frauenfeld and Davis, 2003; Trenberth et al., 2007). Recent studies predict a future for this region marked by subtropical-tropical anticyclonic subsidence for most of the year, which will clearly imply less precipitation and more torrential rainfall and flooding, plus longer-lasting dry periods (Barcikowska et al., 2018; Zappa, 2019).

The Mediterranean coast of the Iberian Peninsula is no stranger to

\* Corresponding author.

E-mail address: [david.corell@uv.es](mailto:david.corell@uv.es) (D. Corell).

<https://doi.org/10.1016/j.atmosres.2023.106695>

Received 4 November 2022; Received in revised form 24 February 2023; Accepted 26 February 2023

Available online 1 March 2023

0169-8095/© 2023 The Author(s). Published by Elsevier B.V. This is an open access article under the CC BY-NC-ND license (<http://creativecommons.org/licenses/by-nc-nd/4.0/>).

this problem and the scientific community has traditionally paid attention to the effects that climate change may have on it. Although the first studies carried out on precipitation evolution in the second half of the 20th century for the entire Spanish territory did not show any generalized trend of change (Castro et al., 2005; Serrano et al., 1999), a study in the 21st century affirmed that there was sufficient evidence for changes (Bladé and Castro Díez, 2010). In line with this, Alpert et al. (2002) employed precipitation data from 265 Mediterranean stations for the 1951–1995 period (182 in Spain), and observed significantly more days with the most intense precipitation. These results coincide with those obtained by Goodess and Jones (2002) in a similar study. However, total amounts of rainfall have been reduced by 10–20% for the same period with a statistically significant trend (Piervitali et al., 1998). In recent years, several studies that have resorted to surface databases inform about a negative trend in annual precipitation amounts and wider interannual variability (De Luis et al., 2009, 2011; Miró et al., 2009, 2018).

Headwaters are key sectors of river systems, and a large part of the water in large rivers comes from them (Martínez-Fernández et al., 2013). Their importance increases in regions where water is scarce and rainfall is irregular (Thornes et al., 2009), which is the case on the Mediterranean facade of the Iberian Peninsula. Recent studies carried out in headwater catchments in the Iberian Peninsula, which are slightly or not at all anthropized, report a generalized negative trend in river flows (Martínez-Fernández et al., 2013). In such headwaters, the main factors controlling water flows over time are climatic oscillations, and variations in land use and land cover (Kundzewicz et al., 2007). As precipitation is the main input of the hydrological system in this southeastern sector of the Iberian Range (López-Moreno et al., 2009; Millán et al., 1998), it is essential to analyze its behavior and expected trends because changes in the distribution of water inputs can lead to a discrepancy between water availability and demand (López-Moreno et al., 2004). We ought not to forget that the Mediterranean coast of the Iberian Peninsula is a densely populated area, and with a high level of industrial and agricultural activity, which all imply considerable water use. It is also one of the main tourist destinations in the Mediterranean basin, with intense tourist activity and higher population density in summer months and, thus, water use increases during this season. It is, therefore, an area where water is considered a scarce resource, whose optimal management is essential for the future of this region. It should be noted that the water that originates in this sector is used by the population of the Valencian Community and the Region of Murcia, two densely populated regions. These regions very much depend on the flows of the Júcar, Turia and Tagus rivers (through the artificial Tagus-Segura Water Transfer Canal). Hence the importance of this study.

In order to carry out a robust and reliable analysis of precipitation trends, it is essential to work with meteorological networks with long homogeneous series. This is essential in mountainous areas, such as rivers' headwaters, where a dense network of rainfall gauges is necessary. Here the terrain is complex, which can bring about significant variations in precipitation volumes between spatially proximate areas. In the Iberian Peninsula, several studies have been carried out on changes in precipitation in some headwaters and their influence on river runoff, but with no conclusive results about the influence of precipitation. Using data from 23 weather stations for an area of 10,646 km<sup>2</sup> during the 1945–1995 period, Gallart and Llorens (2004) observed a negative trend in precipitation in the northern headwaters of the Ebro river basin in 15 rainfall series (four were statistically significant), while the observed trend was positive in the other stations. López-Moreno et al. (2010) analyzed the precipitation trend in the whole Ebro river basin using data for 1955–2006 from 217 stations, and found negative trends in winter and spring in northern headwaters. In the Duero river basin headwaters (northern half of the Iberian Peninsula), and using data for 40 years (1963–2002) from 11 rain gauges and an area of 552 km<sup>2</sup>, no significant negative trends in annual precipitation totals were detected (Morán-Tejeda et al., 2010). However, Miró et al. (2018)

analyzed temporal rainfall evolution over the whole territory of the Júcar and Segura basins with data from 1955 to 2016 and a dense network of stations (890 series). These authors reported statistically significant negative trends in moderate rainfall (10–40 mm) at the stations located in the headwaters of both basins (Miró et al., 2009, 2018).

Drought is the main natural hazard in Spain in terms of economic and environmental impacts (Vicente-Serrano et al., 2017). Future forecasts in the climate change context justify the importance of studying droughts in Spain (Clemente et al., 2018). Drought indicators are extremely important tools for preventing socio-economic impacts, especially in regions where variability in the precipitation regime is wide. This is the case of the Iberian Peninsula, which is located in a climatic transition area where drought conditions have a differentiated pattern due to its intermediate location between a temperate and a subtropical climate (Peña-Gallardo et al., 2016). By considering this issue, several authors have studied drought evolution in the Iberian Peninsula (García-Herrera et al., 2007; Lana et al., 2001, 2006; Vicente-Serrano et al., 2004; Vicente-Serrano, 2006). However, very few studies have focused on analyzing headwater droughts. Only Lorenzo-Lacruz et al. (2010) have studied drought in detail in the Tagus river headwaters using standardized indices that allow comparisons to be made to other studies, such as the SPI (Standardized Precipitation Index) and the SPEI (Standardized Precipitation Evapotranspiration Index). Vicente-Serrano et al. (2010) compared both indices in detail and highlighted that, for a global warming scenario, employing the SPEI is more appropriate because temperature is taken into account.

The aim of this work is to analyze annual and seasonal trends, the evolution of dry and wet periods, changes in the precipitation structure and drought evolution in a key sector of the Iberian Peninsula, the headwaters of the Júcar, Turia and Tagus river basins and in several tributaries of the Guadiana and Ebro rivers, which are water supply areas of large sectors of the east coastal and central peninsular areas. In turn, all the water that feeds the most important river transfer in Spain, the artificial Tagus-Segura Water Transfer Canal, comes from this area, and is used to supply several regions of SE Spain, one of the driest areas in Europe with regular water deficit due to low annual rainfall volumes, irregular rainfall, and high agricultural and urban water demands. Meteorological data from a dense network of meteorological stations over a 70-year period are employed to obtain detailed information about the changes that have occurred in this key sector of the water system. The thus-obtained results will provide valuable information for decision makers to implement future hydrological planning in the region, and all this in the climate change context, and by always assuming that the obtained trends are maintained in the future.

## 2. Material and methods

### 2.1. Study area

A rectangular area of the eastern inland area of the Iberian Peninsula between latitudes 0.75°W and 3°W and 39.5°N and 41.25°W was selected as the study area, whose surface area covers 37,030 km<sup>2</sup> (approximately 189 km wide and 194 km high). This area includes the agricultural districts of *Serranía Baja*, *Serranía Media* and *Serranía Alta* in the province of Cuenca; *Molina de Aragón* in the province of Guadalajara; *Serranía de Albarracín* in the province of Teruel; *Rincón de Ademuz* in the province of Valencia (dashed line, Fig. 1). A decision was made to widen the area formed by the agricultural districts to include in the study the adjacent areas where important rivers originate, such as the Mijares, Alfambra (tributary of the Turia river), Jiloca and Huerva (tributaries of the Ebro river) to the east, and Guadiela, Tajuña and Henares (tributaries of the Tagus river) and the Cigüela and Záncara (tributaries of the Guadiana river) to the west.

It is, therefore, an area with a complex hydrological system and one of vital importance for the recharge of headwaters from some of the most important rivers in the Iberian Peninsula. At the same time, four

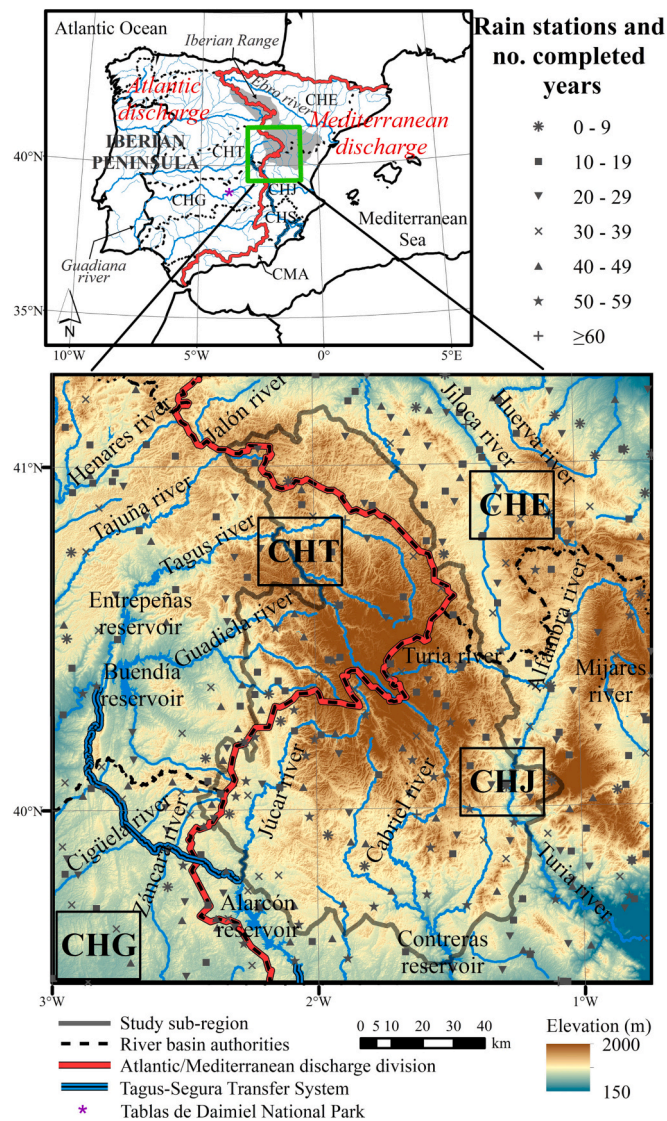


Fig. 1. Study area. Pluviometric stations are represented by symbols according to the number of the originally available completed years.

different hydrographic basins converge on it: the Ebro, Guadiana, Júcar and Tagus (Ebro Hydrographic Confederation (CHE), Guadiana Hydrographic Confederation (CHG), Júcar Hydrographic Confederation (CHJ) and Tagus Hydrographic Confederation (CHT), respectively). In turn, all the water used in the artificial Tagus-Segura Water Transfer Canal is extracted from this area and employed to supply not only areas in the SE Iberian Peninsula belonging to the Segura Hydrographic Confederation (CHS) and the Andalusian Mediterranean Basin (CMA), but also supplementary irrigation to the Tablas de Daimiel National Park located in CHG. Therefore, it is one of the most important watersheds in the Iberian Peninsula for being the place where water flows to the Mediterranean Sea via the rivers belonging to CHE and CHJ, and to the Atlantic Ocean via the rivers corresponding to CHG and CHT. In CHE, and with a selected surface area of 8027 km<sup>2</sup>, there are two Ebro river tributaries, the second longest and most abundant in the Iberian Peninsula, such as the Huerva and Jalón rivers, along with the Jiloca river, a tributary of the latter. In CHJ, with an area of 15,081 km<sup>2</sup>, we find the Turia river and its tributary the Alfambra river, the Júcar river, its tributary the Cabriel river and two of its reservoirs (Alarcón and Contreras), as well as the Mijares river. In CHG, with an area of 3581 km<sup>2</sup>, there are the Cigüela and Zancara rivers, both of which are tributaries of the Guadiana river (the fourth longest river in the Iberian Peninsula). Finally in

CHT, with an analyzed surface area of 11,224 km<sup>2</sup>, there are the Tagus river, the longest river in the Iberian Peninsula, several of its tributaries (Henares, Tajuña and Guadiela rivers) and two of its reservoirs (Entrepeñas and Buendía). The artificial Tagus-Segura Water Transfer Canal starts downstream of these two reservoirs and, after passing through the Alarcón reservoir (CHJ), it supplies water to areas of SE Spain in times of drought with up to a maximum of 650 hm<sup>3</sup>/year (600 for both CHS and CMA, and 50 for CHG) (Melgarejo Moreno and López Ortiz, 2020; Morales Gil et al., 2005). This can have been, and still is, a source of conflict between governments and the population living in the affected regions (Gil Olcina, 1995).

The selected study area is located in the eastern inland area of the Iberian Peninsula, specifically in the SE part of the Iberian Range, and is one of the most important mountain systems of the peninsula. This area has a complex orography and a dense network of rivers that originate there. The maximum altitude exceeds 1900 m in the central part of the study area, drops to 1000 m as we move away toward its edges, and its lowest point is reached in the SE, where it enters the littoral plain of the Turia river.

The study area acts as an island with considerable rainfall in the Iberian Peninsula, with values between 800 and 1000 mm/year in its central part, which coincide with the highest altitude areas. As we move away from the center, rainfall lowers to values between 300 and 500 mm (Fig. 2). Regarding the number of rainy days, the maximum number in the study area is also for the central part, with an average between 75 and 100 days/year, which lowers to 50–75 days/year in the remainder, except for a small area in the SE zone with lower values of 25–50 days/year. In the Iberian Peninsula, the geographical arrangement of the relief, together with altitude, brings about islands with very high precipitation maximums in relation to their surroundings. (Martín-Vide and Olcina-Cantos, 2001), which is the case in this sector. Except for the N-NW Iberian Peninsula with more rainfall, the selected area is one of these singular spots where rainfall is relatively high compared to neighboring areas, which reveals its hydrological and environmental importance.

## 2.2. Daily rainfall database

For this study, 353 series belonging to the State Meteorological Agency (AEMET) were selected for the 1952–2021 study period. The criteria for starting in 1952 was due to the few rainfall stations with data before that year. This meant that the statistical methods used for gap filling and homogenization no longer have dense enough spatial information to ensure the estimated data's sufficient reliability. Fig. 3 shows the stations availability from the beginning to the end of the study period (line chart). In the starting year of the rainfall series, the number of stations came close to 100, but this figure dropped close to half in previous years. The maximum number of stations appeared in the 1970s, with approximately 250, a number that has now dropped to <100. Fig. 3 also shows the number of stations according to the number of years with all the valid original daily observations (bar chart). It illustrates how most of the used rainfall stations (59%) present rainfall series with fewer than 30 years of complete observations. Only seven stations have observations with >60 complete years, which represents 2% of the total. All the selected stations have >8 complete years of original observations. This means that the subsequent gap filling and homogenization processes are valid.

As this is a network of manual stations, raw data have numerous gaps and inhomogeneities. So statistical methods had to be applied to obtain the finally used database, which solved these problems. The methodology described in Miró et al. (2017), which follows the NLP-CA-EOF-QM (non linear principal component analysis-empirical orthogonal functions-quantile mapping) gap filling method, was applied to fill the data and obtain the complete series for the 1952–2021 period. This procedure performs the gap filling of missing data using the meteorological information of the remaining stations from the fundamental



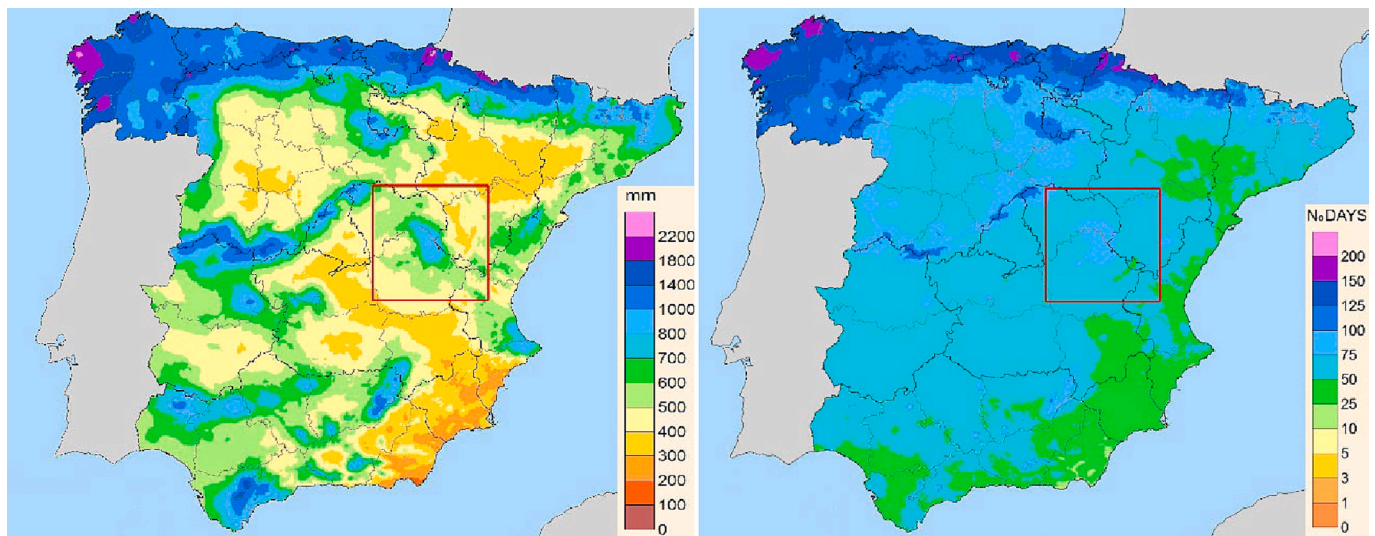


Fig. 2. Mean annual precipitation (left) and mean annual number of rainy days  $\geq 1$  mm (right) for the reference 1981–2010 period (State Meteorological Agency (AEMET), 2018).

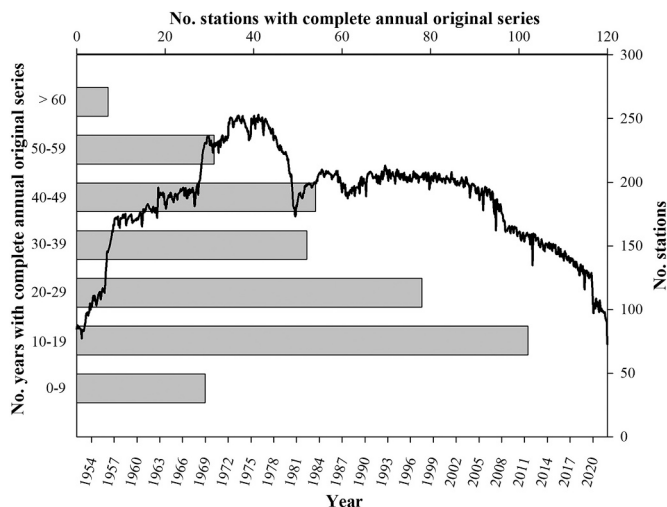


Fig. 3. Evolution of the number of available stations over the study period (line, right and bottom axis) and number of available stations based on the number of years with complete annual original series for the 1952–2021 period (horizontal bars, left and top axis).

variability components obtained by dimensionality reduction by employing all the spatial information available in each time step and the estimation of missing data by a non linear process with an inverse neural network (Miró et al., 2017). The validation process estimated low values for the Mean Absolute Error and Root Mean Square Error (1 and 3 mm), correlations close to 1 ( $> 0.9$ ) and bias close to 0. Likewise, the cumulative distribution function and wet/dry events ratio were preserved in the estimated data (Miró et al., 2017). Furthermore, according to Miró et al. (2017, 2018), the minimum series length to correctly constrain the statistical relations with the information available from neighboring series was 5 years, but a 9-year one for the optimal estimation of extremes (Miró et al., 2017, 2018). Following this criterion, all the series with  $> 8$  years of observed daily data were used in the process, which were reconstructed to the full 1952–2021 period with homogeneity and no gaps. This allowed the spatial-temporal analysis to be continuous; i. e., without changes due to discontinuities in the spatial-temporal information available for the full 1952–2021 period. It was noteworthy that the ACMANT method (ACMANTv3.0-ACMANTP3day; Domonkos,

2014, 2015) was followed in the homogenization process of the already filled precipitation series.

Although the present study was limited to a specific area of interest, the gap-filling homogenization process was carried out using all the spatial-temporal information available in the entire eastern peninsular and Mediterranean basin. This involved 4780 daily rainfall series from the AEMET network covering the complete Ebro, Júcar and Segura basins, the basins of Catalonia and the Balearic Islands, the Andalusian Mediterranean Basins, as well as the entire eastern half of the Tagus, Guadiana and Guadalquivir basins. This database was called the “Complete Daily Rainfall Database for a High-Resolution Analysis in the eastern Iberian Peninsula: 1952–2021” (CDRD-HR-EIP-1952–2021). In the study area covered by the present study, 353 complete series from this database were used. This resulted in an average density of approximately one station every 100 km<sup>2</sup>.

### 2.3. Methodology to analyze trends and observed changes

For the trend analysis of the time series throughout the study period (1952–2021), non parametric procedures were applied to detect the existence of statistically significant trends in each one. For this purpose, the following statistical parameters were calculated:

- The Mann-Kendall trend test (Kendall, 1962; Mann, 1945) to determine the presence of a statistically significant trend. It was tested according to statistical significance levels  $\alpha = 0.01$ ,  $\alpha = 0.05$  and  $\alpha = 0.1$ , and plotted on result maps (filled point (confidence  $> 99\%$ ), half-filled point ( $> 95\%$ ), circle-cross point ( $> 90\%$ ) and unfilled gray point when a non significant trend was obtained). Blue on the map represents positive trends, while red denotes negative ones.
- The annual Sen slope of change obtained for each station. This includes: 1) the annual Sen slope (absolute change); 2) the annual relative change derived from the Sen slope, which allows the relative importance of change in normal precipitation to be appreciated regardless of its absolute value being high or low. Both results were spatially interpolated and graphically displayed.

In addition to the above, climate normals were obtained for two different periods lasting  $> 30$  years. For this purpose, the sample was divided into two 35-year periods (1952–1986 and 1987–2021) and the differences in precipitation between them were calculated. The results were spatially interpolated and graphically displayed. Although this method does not provide statistical confidence levels like the previous



method does, it allows the changes between the two periods to be simply visualized which, thus, improves the interpretation of the results.

The local polynomial interpolation method, with a resolution of 200 m, was followed to plot the results on maps, which was successfully tested with the precipitation data and was applied to identify a long-range trend, as reported by Wang et al. (2014).

#### 2.4. Precipitation variables tested for changes

The statistical methods described in the previous section were implemented in the following fields related to precipitation:

1. Precipitation volumes and number of days with annual and seasonal rainfall:
  - Trends of annual and seasonal precipitation volumes (Winter: Dec-Jan-Feb, Spring: Mar-Apr-May, Summer: Jun-Jul-Aug, Autumn: Sep-Oct-Nov) for the 1952–2021 period.
  - Spatially interpolated mapping of changes in the annual and seasonal mean precipitation and number of rainy days between the 1952–1986 and 1987–2021 periods.
2. Daily precipitation classified by percentiles.
  - First, the following 25th, 50th, 75th, 95th and 99th percentiles, and the maximum values of each series, were calculated with the daily precipitation data.
  - Second, the daily rainfall data between the 50th and 95th percentiles were classified as moderate rainfall. The following aspects of this type of rainfall were analyzed:
    - i. Spatially interpolated mapping of changes in the annual mean precipitation between the 1952–1986 and 1987–2021 periods.
    - ii. The Mann-Kendall trend test and Sen slope for the 1952–2021 period by grouping all the series into two average series. The first one includes those series with a negative absolute change in total precipitation volumes between the 1952–1986 and 1987–2021 periods. The second one contains those with a positive change. In this case, the annual number of events with rainfall amount falling between the 50th and 95th percentiles and the annual precipitation sum (average per station) for these events are analyzed.
    - iii. Trends of annual precipitation volumes for the 1952–2021 period for each series (stations) separately.
3. Length of dry and wet periods, by considering dry (or wet) periods to be those with two consecutive dry (or wet) days or more. The rule  $\geq 1$  mm distinguishes wet days from dry days (World Meteorological Organization, 2016). The Mann-Kendall trend test and Sen slope (1952–2021) were calculated for the following variables:
  - Annual maximum dry spell duration (as consecutive days).
  - Annual average of dry spell duration (as consecutive days).
  - Annual average of wet spell duration (as consecutive days).

#### 2.5. The drought index: the SPEI

The SPEI (Vicente-Serrano et al., 2010) is a well-known index, and is similar to the SPI, for measuring drought status in a given area by allowing comparisons to be made between climates. Like the SPI, the SPEI can be calculated on several time scales of response to drought of natural systems or dependent socio-economic activities (1 month to 48 months, or more). Yet the SPEI takes into account not only precipitation, but also potential evapotranspiration (PET) in its calculation, which is more useful in the climate change context where the additional effect of rising temperatures leads to greater water losses through

evapotranspiration.

The SPEI was originally based on the monthly PET calculation by following relatively simple methods, such as Thornthwaite. Today it can be calculated even on a daily scale with more elaborate PET calculation methods (e.g. Wang et al., 2021). Such calculations on a daily scale allow a more accurate adjustment of the start and end of wet/dry periods.

For the present study, the SPEI was calculated for each point series of the total series employed, and for time windows of 3, 12 and 36 months, as being representative of the short, medium and long terms, and also on a daily basis. As the index is sensitive to the choice of an appropriate probability function toward better performing extremes (Beguería et al., 2013; Stagge et al., 2015, 2017), the method followed to calculate the SPEI was that proposed in Stagge et al. (2015). It is based on using the generalized extreme value distribution, together with daily precipitation and PET.

For the PET calculation, we opted for the McGuinness-Bordne method because daily PET can be calculated with a few additional variables, in this case temperature, because most available stations do not have other variables needed for other methods. This method has been used with good results in the daily PET database covering the UK by Tanguy et al. (2017). It was, therefore, applied for all the available thermo-pluviometric series.

The need for temperature series to calculate SPEI was met in a similar way to that used for precipitation. The same AEMET stations with daily temperature records (thermo-pluviometric) were used (132 stations within the study area). For quality control, gap filling and homogenization, the same rules and procedures already described for precipitation and in Miró et al. (2017) were used, although in this case no adjustment of the dry/wet ratio was required. All the gap filling methods tested in Miró et al. (2017) were now applied to temperatures, but in this case the best filling method was Variational Bayesian PCA -VBPCA- (Ilin and Raiko, 2010) instead of NLPCE-EOF. In this case, for the validation data and after the adjustment to preserve the probability density function (QM), the mean daily error (MAE) in the estimated daily missing data was always  $\leq 1$  °C and the RMSE was always  $\leq 1.4$  °C, an error that becomes negligible ( $< 0.1$  °C) and without bias for the monthly (and annual) averages.

On the one hand, the SPEI results herein presented graphically show full temporal resolution, but by grouping series by different river basin headwaters. That is, the average series is represented for all the series that fall within the headwaters in the river basin of each given river. A graph is, thus, represented for the Tagus (CHT), Ebro (CHE), Júcar (CHJ) and Guadiana (CHG). On the other hand, they are presented in the form of spatial interpolation of the results on a map, where the complete spatial information deriving from all the point series appears (spatially interpolated), but in a more simplified temporal form. In this case, as the SPEI is calculated by considering the entire 1952–2021 period, the change in the average SPEI value over the last 35 years of the series vs. the first 35 years is represented.

A similar representation of the change between both periods is also considered by referring more specifically to the magnitude of the more characteristic dry/wet periods. In this case, the 20th and 80th percentiles of the full data distribution (1952–2021) in all the employed time windows come close to the SPEI values +1 (80th percentile) and  $-1$  (20th percentile) on average. +1 and  $-1$  are frequently indicative levels to signal a wet period or drought when they are exceeded by the index. Therefore, the next step involves calculating the 80th and 20th percentiles for the SPEI distribution (based on the 1952–2021 set), but by initially considering only the data for the first 35 years and then taking only the data for the last 35 years. This allows the mean change between both periods to be plotted as a way to assess the increase or decrease in the frequency of these dry/wet periods.

### 3. Results

#### 3.1. Changes in volumes and number of rainy days

Changes in precipitation volume are studied by two analyses with similar results: a generalized reduction in precipitation over time. The first analysis shows the trends and slopes obtained (1952–2021) for the annual rainfall volumes and appears in Fig. 4 (the top images with all the available stations, while the bottom images only with the rainfall series with at least 40 years of the originally observed data to corroborate the findings). For both cases, this analysis illustrates how negative trends predominate and most are statistically significant at 99%. The second analysis depicts the average annual precipitation for the 1952–1986 and 1987–2021 periods, as well as the difference between both periods, as shown in Fig. 5 (top images). This analysis also indicates generally reduced precipitation in the study area, except for the extreme SE (toward littoral areas), where there is one area showing an increase. When observed in detail, differences in the four river basins appear. In CHT, negative trends clearly dominate and a generalized decrease in precipitation volume is observed. In fact, 63 out of the 80 analyzed stations reveal statistically significant and negative trends. In 40 of them, confidence is as high as 99%. At the same time, the slope throughout the area is negative, with more pronounced significant losses in the area bordering CHJ (from  $-3$  to  $-5$  mm/year). In turn, it is the basin with the most marked reduction in average precipitation ( $-81$  mm), and where

reduction obtains the highest percentage in relation to the annual average ( $-12.1\%$ ). In its central part, and coinciding with the highest altitude areas, there is an area with more pronounced decreases and loss values of  $>75$  mm, which exceed 200 mm at some points. There are stations in this basin where the reduction in precipitation represents  $>25\%$ . A similar behavior is observed in CHG, with 75% of the analyzed stations showing a negative and statistically significant trend, a negative slope and with general decreases throughout the area, with losses exceeding 48 mm in most of the area. The average reduction in this basin is 56 mm. Behavior in CHJ is not homogeneous and negative trends do not predominate and represent 36% of the analyzed stations. This means that, although the basin obtains an average decrease of  $-25$  mm, there are also areas where increases were detected, which are located in the extreme SE where the basin reaches its lowest altitude. In this basin, the drop in precipitation predominates in its western part and the area linking CHT stands out, which coincide with the Atlantic-Mediterranean watershed, for obtaining very pronounced significant losses of up to 200 mm/year at some points. In slope terms, a clearly negative southeast-to-northwest gradient is observed. Finally in CHE, although the stations with negative trends only represent 39% with no positive trends in the whole basin, a general decrease is also observed throughout the area, albeit with smaller losses and decreases between  $-5$  and  $-28$  mm predominate. Losses increase in the areas bordering CHT, with peaks above  $-75$  mm at some points. The losses in this area represent 6.6% of the total.

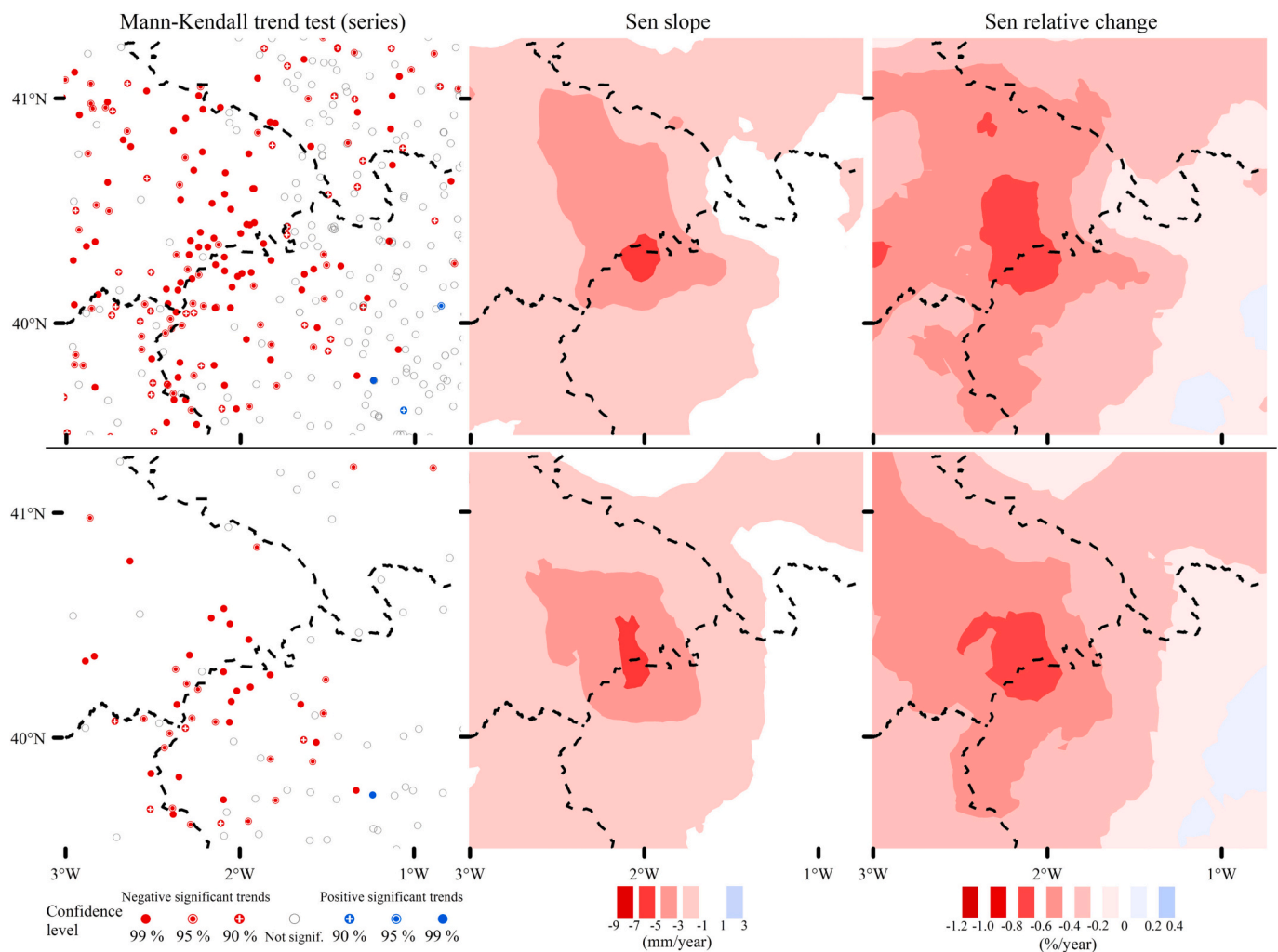


**Fig. 4.** Significant trends (1952–2021), annual slopes and relative (%) slopes for annual rainfall volumes. Top image, using all the stations. Bottom image, the same analysis, but using the only stations with  $>40$  years of real observed data.

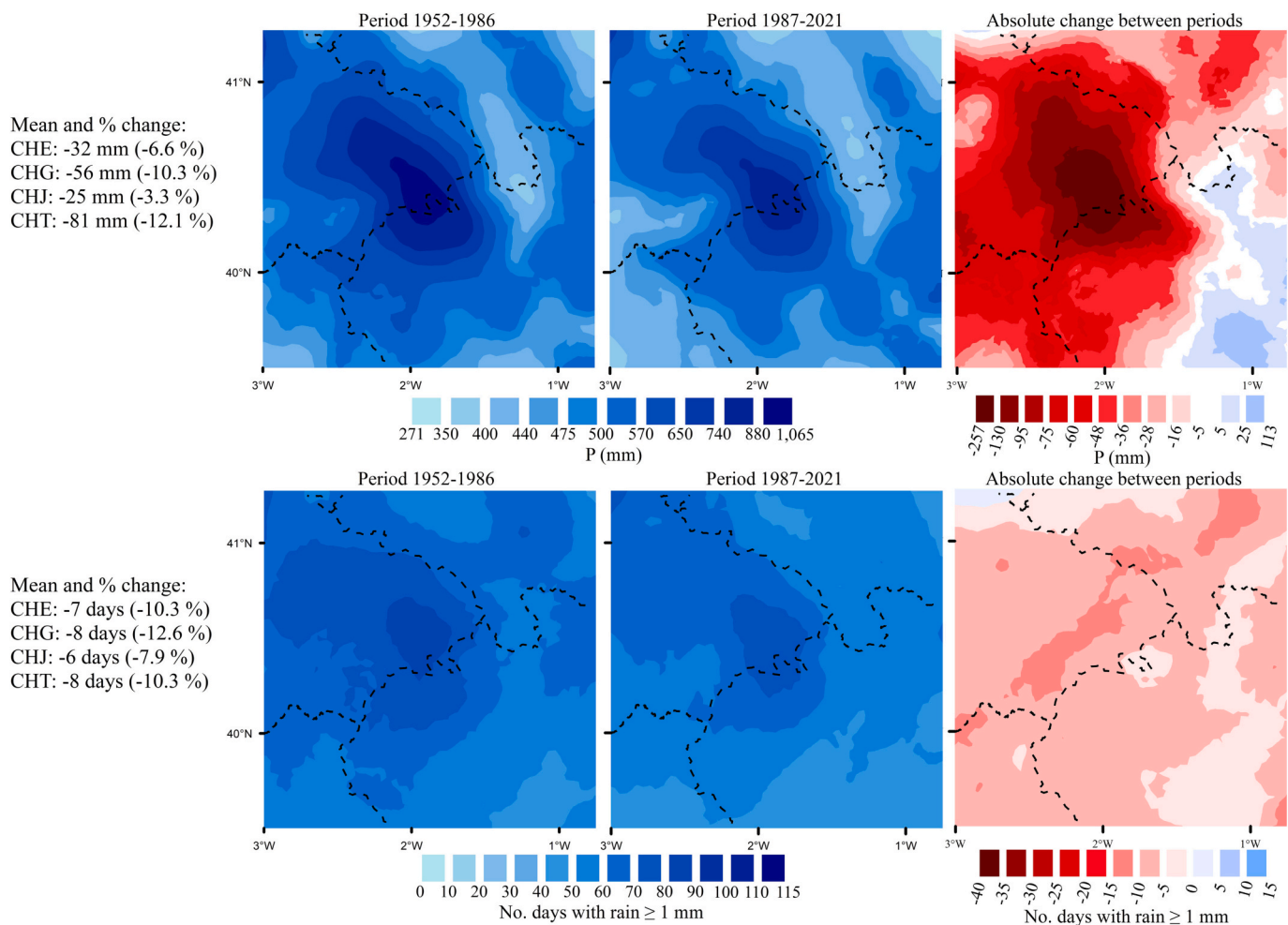


**Fig. 5.** Mean annual precipitation (top images) and mean annual number of rainy days ( $\geq 1$  mm) (bottom images) for the 1952–1986 (left images) and 1987–2021 (center images) periods, and absolute change between periods (right images). On the left, the mean and relative importance of these changes.

Similarly, a generalized drop in the number of rainy days appears throughout the study area. The average reduction in precipitation is approximately 10%. As Fig. 5 (bottom images) shows, the area with the most rainy days, which occupies the eastern part of CHT and reaches some CHJ sectors during the 1952–1986 period and with an average number of rainy days between 80 and 90, maintained its shape during the 1987–2021 period. However, the number of rainy days falls within the 70–80 interval, which implies a reduction. For the rest of the analyzed territory, the spatial distribution of number of rainy days remains, albeit with a reduction of 6–8 days of rainy days between both periods. A slight increase in number of rainy days is seen only in a small area located in the extreme NW of CHT.

### 3.2. Changes in amounts of seasonal rainfall and number of rainy days

Changes in amounts of seasonal rainfall are also studied by two analyses. First, Fig. 6 shows the precipitation trend and slopes obtained (1952–2021) for the seasonal rainfall volumes. Second, the changes between the 35-year study periods are analyzed for each season of the year (Fig. 7 left and center images, and supplementary Fig. S1). Differences appear at distinct times of the year and between river basins. Winter is the season showing the greatest reduction in precipitation (average of  $-24$  mm,  $-13.2\%$  in relative terms) and that with the clearest negative trend, with statistically significant trends in two thirds of the analyzed stations. CHT and CHG are the most affected basins because  $>78\%$  of the values display this trend for both, with the

decrease in seasonal precipitation representing  $22.7\%$  ( $-44$  mm) and  $18.2\%$  ( $-30$  mm), respectively. CHJ ( $-19$  mm and  $-9\%$  in relative terms) with the negative values located in the western part, and CHE ( $-10$  mm and  $-9.5\%$  in relative terms), are the least affected basins. During this season, there is no station with a positive trend for any studied basin. The slope map shows precipitation general loss throughout the study area, with more importance for precipitation in the western part and more incidence in higher altitude areas. Summer reveals similar behavior than winter, although fewer stations show a negative trend and the general decrease is smaller (average of  $-18$  mm), the relative importance of this decrease is greater and represents  $-19.3\%$ . The most affected basins are CHG and CHT, with an average reduction of  $>22\%$  in both and with  $75\%$  of the stations depicting a negative trend in the first case. CHE is the least affected area. Negative trends continue to predominate in autumn, but fewer stations obtain statistical significance than in winter and summer. A slight variation ranging from  $-20$  to  $+20$  mm is noted throughout the area and represents only a  $1\%$  average increase. Spring is the season when the most stations display no statistical significance. However, there are a considerable number of stations with a positive trend, which are located mostly in the SE part of the study area (CHJ). In this case, only CHT and CHG show decreased average precipitation between periods.

A generalized decrease in the number of rainy days takes place in winter, summer and spring, but is more important on some (Fig. 7 right images and supplementary Fig. S2). Winter and summer are the most affected seasons, with an average decrease of  $17\%$  in relative terms for



both. The most affected basin is CHG in summer and winter, and in CHT for winter, with reductions in the number of rainy days of around 20%. In spring, reductions throughout the territory are also generalized, but with smaller amounts and of relative importance ( $\approx 5\%$ ) than in winter and summer. In autumn, an alternation in areas of losses and gains occurs. This means that variation is, on average, almost non-existent ( $\pm 0.2\%$ ) in the study area on the whole.

### 3.3. Changes according to precipitation type classified by percentiles

In order to find out how precipitation behaves in the study area, the box-whisker diagram of the 25th, 50th, 75th, 95th and 99th percentiles, as well as the maximum value of the series, of the daily precipitation values for all the stations in the study area for the 1952–2021 period is represented (Fig. 8). Likewise, to know the importance of precipitation according to intensity, Fig. 9 represents the percentage of the total accumulated precipitation for the 1952–2021 period of certain precipitation intervals according to the 25th, 50th, 75th, 95th and 99th percentiles.

As Fig. 8 depicts, the 25th and 50th percentiles represent weak or very weak precipitation, with average values of 2–5 mm/d. This type of precipitation is of very little importance for the hydrological system because, in some cases, water does not reach soil or evaporates before infiltration occurs. At the same time, its importance for total precipitation is slight and accounts for only 16% of the total (Fig. 9). Above the 50th percentile and up to the 95th percentile, rainfall lies mostly between 10 and 40 mm/day. These figures represent moderate rainfall, which is the most usable by the hydrological system. At the same time, the importance of rainfall between these percentiles represents 61% of the total recorded rainfall, and is the most representative set of the study area. Thus the analysis should focus on this type of rainfall.

Fig. 10 represents the average annual precipitation between the 50th and 95th percentiles for the 1952–1986 and 1987–2021 periods, as well as the difference between both periods (top images). In turn, the same study is carried out using only the precipitation series with at least 40 years of the originally observed data (bottom images). As this figure shows in both cases, precipitation reduces throughout the study area, except in the extreme SE, where some areas show no changes and slight increases. The area with the greatest losses lies between CHT and CHJ, and stations obtain decreases of  $>150$  mm. This area extends over a large part of the CHT territory, where reductions are generalized, and also the western area of CHJ, which covers a smaller extension in this basin. In fact, losses become less significant as we move eastward and there are even increases in the extreme SE that sometimes exceed 65 mm. In CHG and CHE, loss of precipitation spreads throughout their territory. The analysis carried out with the stations containing at least 40 years of the originally observed data provides a distribution of precipitation during both periods. Its variation is similar to that obtained by the study of all the stations, which confirms the obtained results.

However, the results obtained in the above analysis may be questionable if the high interannual irregularity of the precipitation is considered. But by grouping the stations according to their precipitation balance between the two periods, and by analyzing the complete average series (1952–2021) of each group separately, new information emerges refuting a scenario of positive changes for the second group, especially when considering the number of moderate events. For this purpose, Fig. 11 separates the rainfall stations with precipitation loss records between periods 1952–1986 and 1987–2021 from the top right image of Fig. 10, which are 269 stations (76% of the total number of stations), and analyses the trend in precipitation volumes and the number of events between the 50th and 95th percentiles (upper figure). Likewise, the same analysis is run with the stations with a recorded increase in rainfall (lower figure), which are 84 stations (24% of the total), and the behavior of both types of stations is compared. As Fig. 11 depicts, there is a statistically significant negative trend for the stations showing an absolute negative change between periods in terms of both

volume and the number of events. However, for the stations with an absolute positive change, no significant trend is observed in increased rainfall volume terms, while a significant negative trend appears (99% confidence) for the number of events, indicating a lower frequency of rainy days at these stations as well.

In addition, the moderate precipitation trend has also been analyzed for all pluviometric stations and it has been found to be decreasing throughout the study area, with more than half the analyzed stations showing statistical significance (supplementary Fig. S3). The behavior in all the analyzed basins is similar, with a dominant negative trend in most of their territory. In CHT, the stations with a statistically significant negative trend represent 64%, but 50% in CHJ, while CHG and CHE take intermediate values. In CHJ, four of the only five stations display a significant positive trend for precipitation. According to the analysis of the stations with  $>40$  years of real observed data, the obtained percentages are similar, with  $>50\%$  of them showing significant and negative trends, which validates the analysis with all the stations. The slope maps indicate the area between CHT and CHJ being that most affected by reductions, along with small areas in the watershed of the different basins. In contrast, the least affected area lies to the east of the study area and covers the areas that lie to the east of CHJ and south of CHE.

### 3.4. Changes in dry-wet spell duration

Fig. 12 shows the trend and absolute change in the maximum dry spell duration, the annual average dry spell and the annual average wet spell over the 1952–2021 period. This figure depicts a slightly increasing maximum dry spell duration trend, albeit with no clear predominance (upper figures). The stations with a positive trend represent 20% of the total, while 6% indicate decreases. In contrast, the map containing the observed absolute change (right) shows a slightly increased maximum duration over most of the territory, together with certain isolated spots with some decreases. At some analyzed stations, increases are of 30 days between the beginning and end of the study period. The annual average dry spell shows a clearly generalized trend of increasing duration (central figures). Approximately half the analyzed stations obtain statistically significant positive trends in all the basins for rainfall, and CHE has the highest percentage of them all (60%). In turn, the map of changes between the beginning and end of the period depicts a general prolonged dry spell duration throughout the study area, except for some isolated small spots. All the basins present stations with increases of  $>4$  days per year, which exceed 8 days in CHJ. Regarding the wet spell duration trend (lower figures), stations with decreases clearly dominate and account for 75% of the total. This percentage even exceeds 90% in CHG, where all but three of the analyzed stations show a statistically significant negative trend. Therefore, the map of changes (right) reveals a general decrease in the whole study area. At some analyzed stations, decreases of  $>50$  days of wet spell duration are recorded.

### 3.5. Changes and trends in the SPEI index

Fig. 13 shows the difference between the 1952–1986 and 1987–2021 periods for the 20th (upper figures) and 80th (lower figures) percentiles of the daily SPEI values on 3-, 12- and 36-month time scales (the 20th and 80th percentiles value for each period appear in the supplementary figs. S4, S5 and S6). The variation between both periods widens depending on the time scale used in the analysis. Thus on average, on the 3-month time scale, the decrease in SPEI for the entire study area is about 21% for both percentiles. However for the longest time scale (36 months), the average differences are 150% (20th percentile) and 72% (80th percentile), and are 50% for the 12-month scale. So all of them obtain lower SPEI values. When analyzing basins separately, major differences appear. Basins CHE, CHG and CHT show generalized decreases in all their areas for all the calculated time scales. Of them all, the CHT basin stands out with marked decreases in its SPEI values,

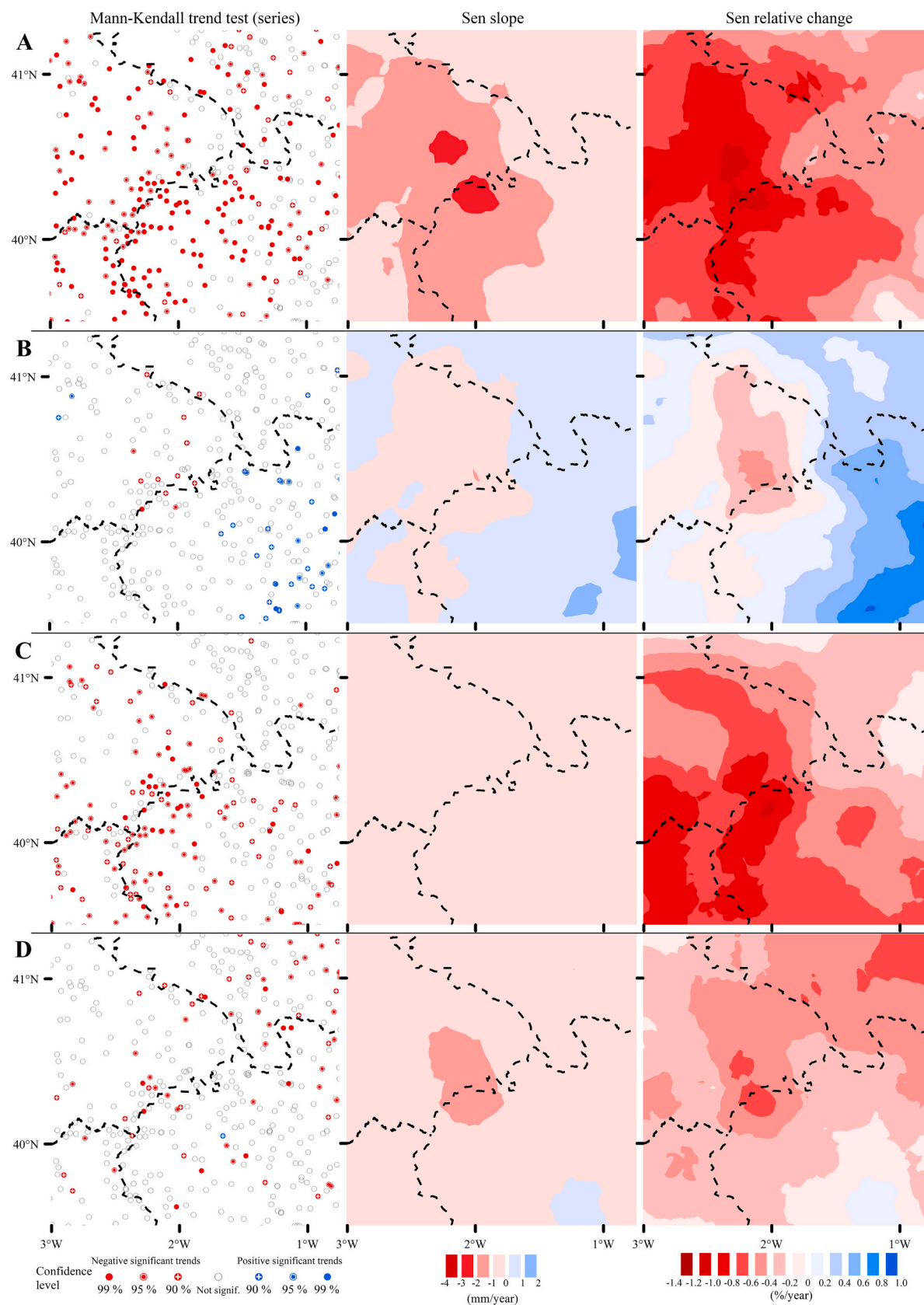


**Fig. 6.** Significant trends (1952–2021), annual slopes (mm) and relative (%) slopes for seasonal amounts of rainfall. A (winter), B (spring), C (summer) and D (autumn) trends.

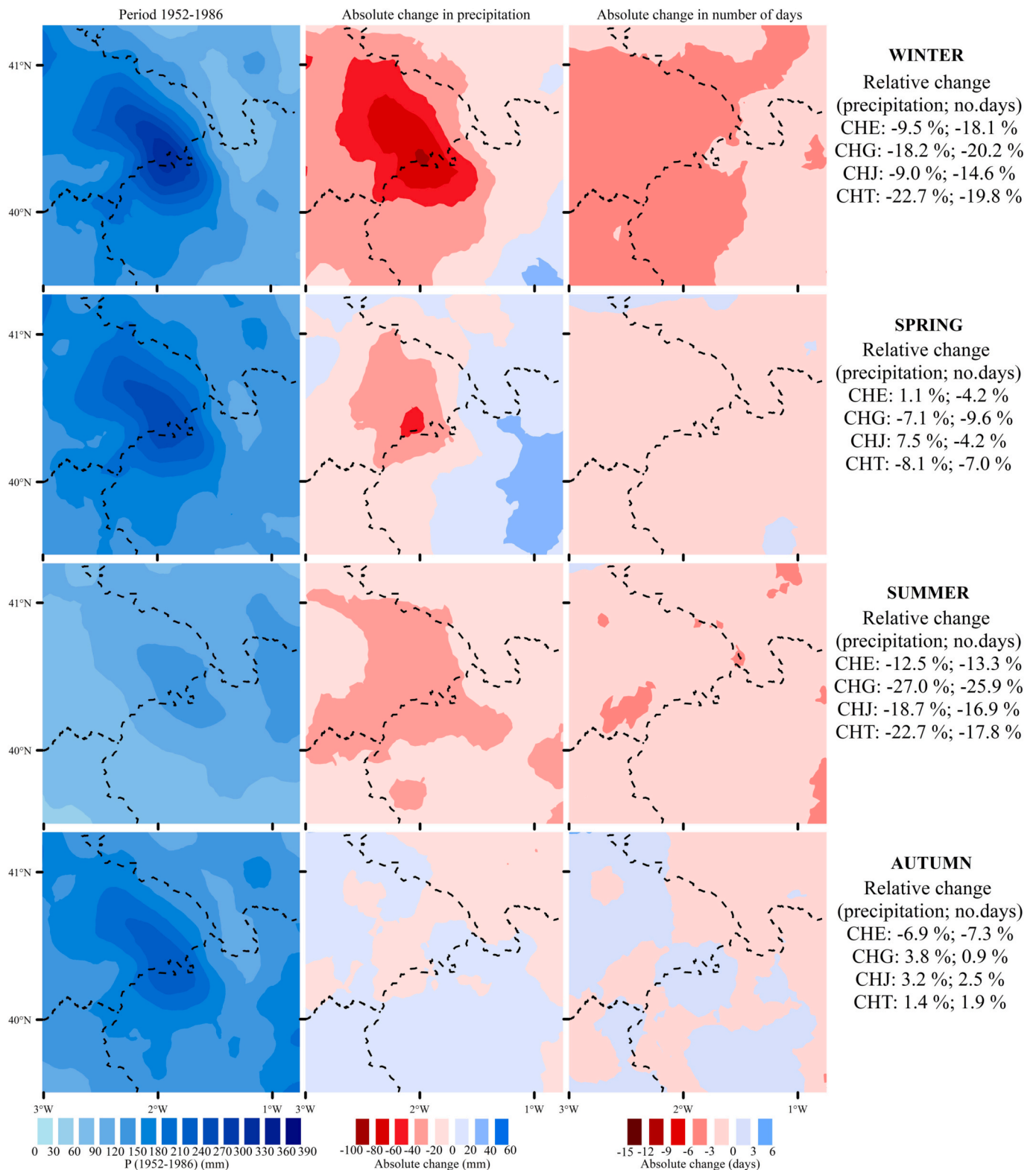


**Fig. 7.** Seasonal mean precipitation for the period 1952–1986 (initial precipitation) and absolute change in seasonal mean precipitation and seasonal mean number of rainy days ( $\geq 1$  mm) between the periods 1952–1986 and 1987–2021. On the right, the relative importance of these changes.

especially in the southern area that coincides with the watershed. For the 36-month time scale and the 20th percentile, the decrease observed in the SPEI value for this basin exceeds 200% and is 89% for the 80th percentile. On the whole, the SPEI values for CHJ drop on the three analyzed scales and for both percentiles, but behavior is not homogeneous throughout the area. In the area close to CHG and CHT, the

drought index values significantly lower, similarly to those observed in the surrounding areas of the other basins. In the extreme SE, some areas obtain slightly higher SPEI values.

The SPEI trend is analyzed on the same time scales (3, 12 and 36 months) over the 1952–2021 period and the absolute change predicted by Sen slope was calculated (supplementary Fig. S7). The stations with a



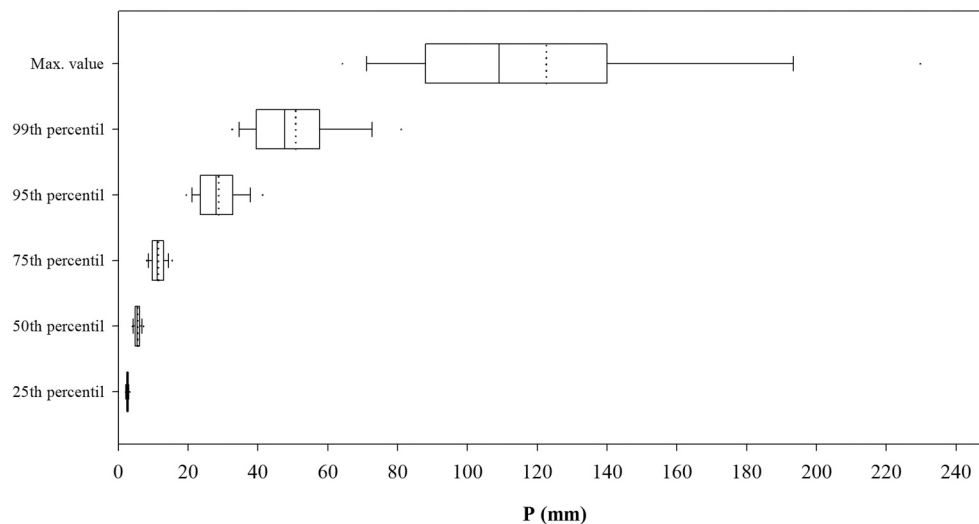


**Fig. 8.** Box-whisker plot of the daily precipitation values representing the 25th, 50th, 75th, 95th and 99th percentiles, and the maximum value of the series, for all the stations in the study area for the 1952–2021 period.

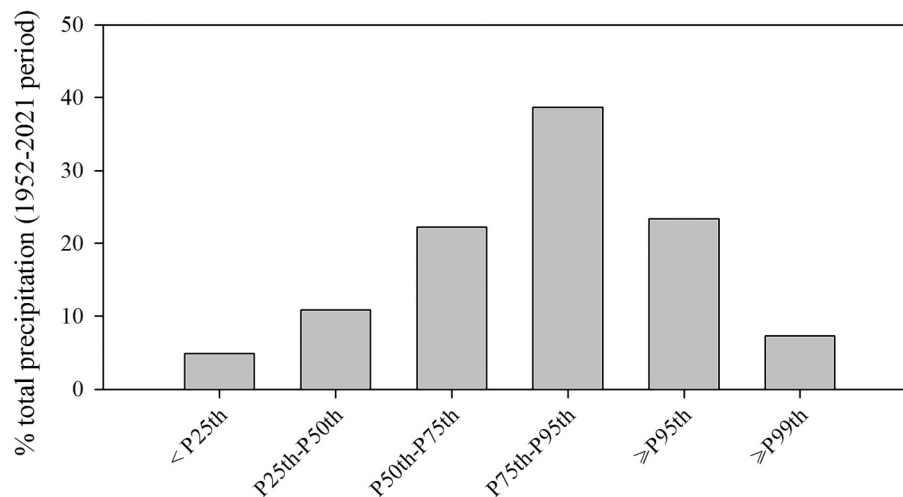


**Fig. 9.** Total percentage of precipitation according to intensity and represented by the 25th, 50th, 75th, 95th and 99th percentiles based on the daily precipitation data from all the stations in the study area for the 1952–2021 period.

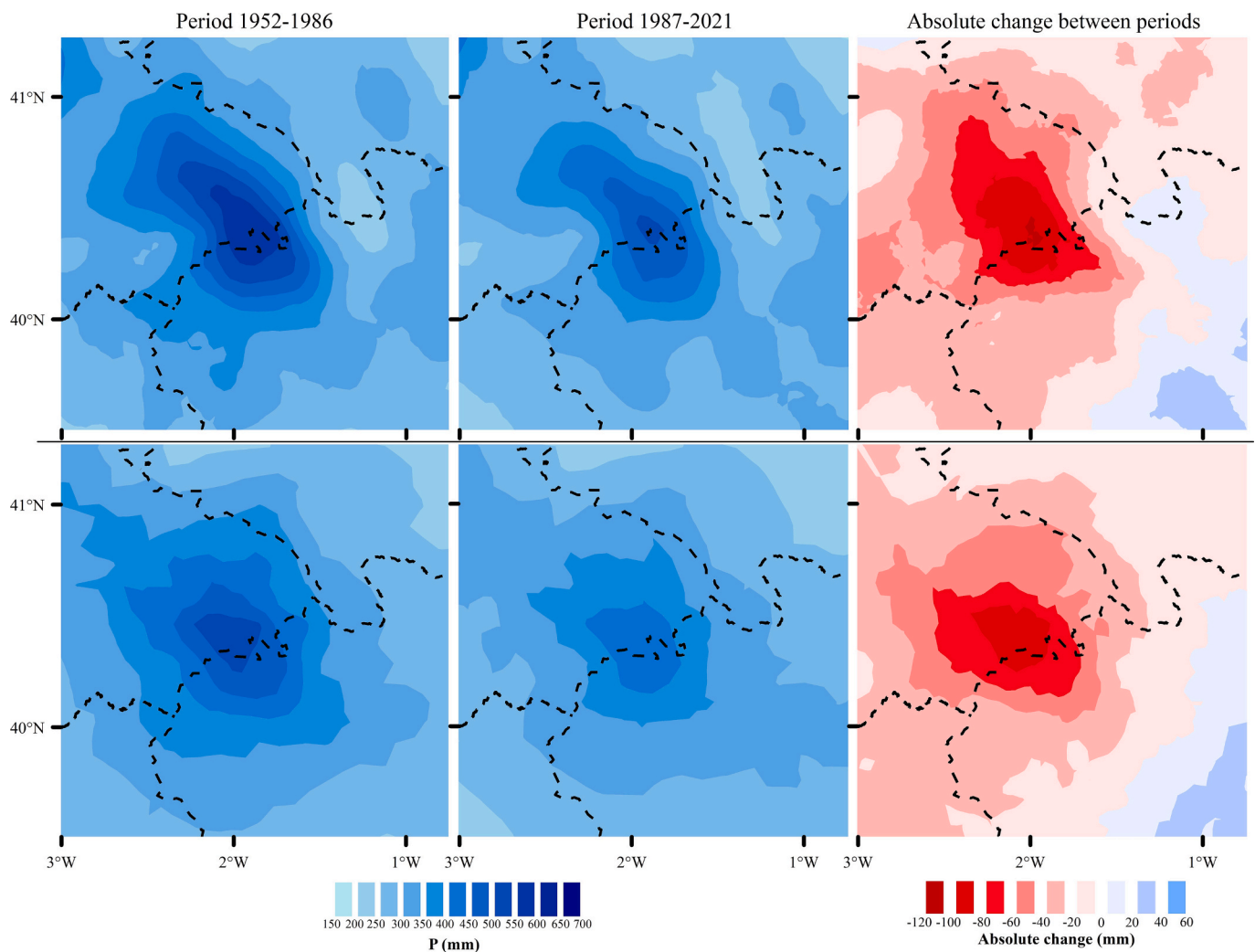
negative trend predominate throughout the study area and on the three time scales. With the 3-month SPEI, 61% of the stations show statistically significant negative trends, with CHG and CHT standing out for obtaining >70%. On the 12-month time scale, the number of stations with a negative trend increases, with 80% excess for CHG and CHT, and a 69% percentage for the whole study area. On the longest time scale, the highest percentage of stations with a statistically significant negative trend is reached, which exceeds 80% in the complete study area, with CHE standing out for obtaining 94%. No positive and statistically significant trends appear for the three time scales. Regarding absolute changes, lower SPEI values predominate throughout the study area and on the three time scales, with some minor differences: (1) the most marked decreases are observed in the area around the watershed separating CHJ, CHG and CHT, with a higher incidence in CHT; (2) positive changes are noted only in the extreme SE of CHJ, where areas show slight increases.

Fig. 14 analyses the time series of the daily SPEI values on the 12- and 36-month time scales by distinguishing among the four studied river basins. For the medium-term drought data (12 months), a very clear predominance of drought periods since the 1980s is noted, while the periods with SPEI values above 0 predominates in previous years. It is

worth highlighting the beginning of the 1990s and most of the years since 2000, when the lowest SPEI values are obtained. This behavior is accentuated with the long-term analysis (36 months). In this case, during the first 30 study years, the periods with positive SPEI values dominate, and are interrupted only by a drought period between 1954 and 1958. However, since the 1980s onward, drought periods predominate and are more pronounced. In the last 40 years, there have been five drought periods, all of which have lasted >4 years, and have been interrupted only by non drought periods lasting <2 years. The situation seen in CHT and CHG is particularly critical, which has been subjected to severe drought since the 2000s. It is in the short-term when drought effects are more difficult to appreciate. In fact, the time series calculated from the 3-month SPEI data (supplementary Fig. S8) shows wide variability in all the basins, and alternating periods with positive and negative SPEI values mainly in recent years.

#### 4. Discussion

With the results herein presented for the new database called “Complete Daily Rainfall Database for a High-Resolution Analysis in the eastern Iberian Peninsula 1952–2021” (CDRD-HR-EIP-1952–2021), the



**Fig. 10.** Annual amounts of precipitation recorded only between the 50th and 95th percentiles: average for the 35-year periods (1952–1986 and 1987–2021) and the absolute change between both periods. Top images, using all stations. Bottom images, same analysis but using only stations with >40 years of real observed data.

overall situation in the study area shows changes toward drier conditions between 1952 and 2021. At the same time, a general decrease in the most effective precipitation to be used by the hydrological system is observed for the following reasons:

- The recorded precipitation volumes are lower during the more recent period (1987–2021) than for the older one (1952–1986), which suggests a trend toward drier and more arid conditions over time. The Tagus river basin headwater (CHT) obtains the most marked decreases in rainfall in the highest areas, which are also those with the highest average annual rainfall. They are also the most affected ones. The same occurs in the Júcar river basin (CHJ), where the area bordering CHT obtains the greatest losses. One of the causes is decreased precipitation volume, which might be due to loss of rainy days throughout the analyzed area. A homogeneous decrease of approximately 10% appears in all the basins.
- Summer and winter are the seasons most affected by reduced precipitation, with losses in some rainfall stations exceeding 120 mm between the two 35-year reference periods and, in some cases, with reductions of almost 50% for all the fallen rainfall. At the same time, climate projections tend to predict a significant reduction in rainfall for forthcoming years (Barcikowska et al., 2018; Grise et al., 2019; Miró et al., 2021; Zappa, 2019), mainly in the months of the above-cited seasons. The most affected basins are CHG and CHT, where 80% of the studied stations show a significant negative trend for

rainfall evolution for the last 70 years. Studies carried out in some headwaters located in the north of the Peninsula, such as the Ebro (López-Moreno et al., 2010), also show negative trends for winter and spring according to data from the 1955–2006 period and from 217 stations. For the CHJ basin, similarly significant downward trends have been detected in the headwaters and inland of the basin, but not in coastal and pre-coastal areas (Miró et al., 2018). In addition, climate projections for the region foresee that these trends will continue and become profounder. Thus in accordance with Miró et al. (2021), change scenarios are projected for the CHJ basin that, through statistical downscaling on CMIP-5 GCMs, affect a greater reduction in precipitation in the headwaters and inland of the basin (in contact with the other study basins) than on the littoral fringe. These projected changes (CHJ-interior) are also greater in spring, winter, and also summer, with decreases of >20% and up to 30% in headwaters. Similarly, the projections reported by Todaro et al. (2022) for the CHJ also foresee marked decreases in the spring (24%) and autumn (10%) precipitations for three future short-term (2021–2040), medium- (1941–2060) and long- (2076–2095) term periods and two emission scenarios: moderate RCP4.5 and higher forcing RCP8.5. However, they indicate an increase in the short-term summer precipitation for RCP4.5 (+7.5%). For CHG, the results fall in line with those obtained here with significant decreases in the summer (61%) and autumn (35%) precipitations for all periods and scenarios.

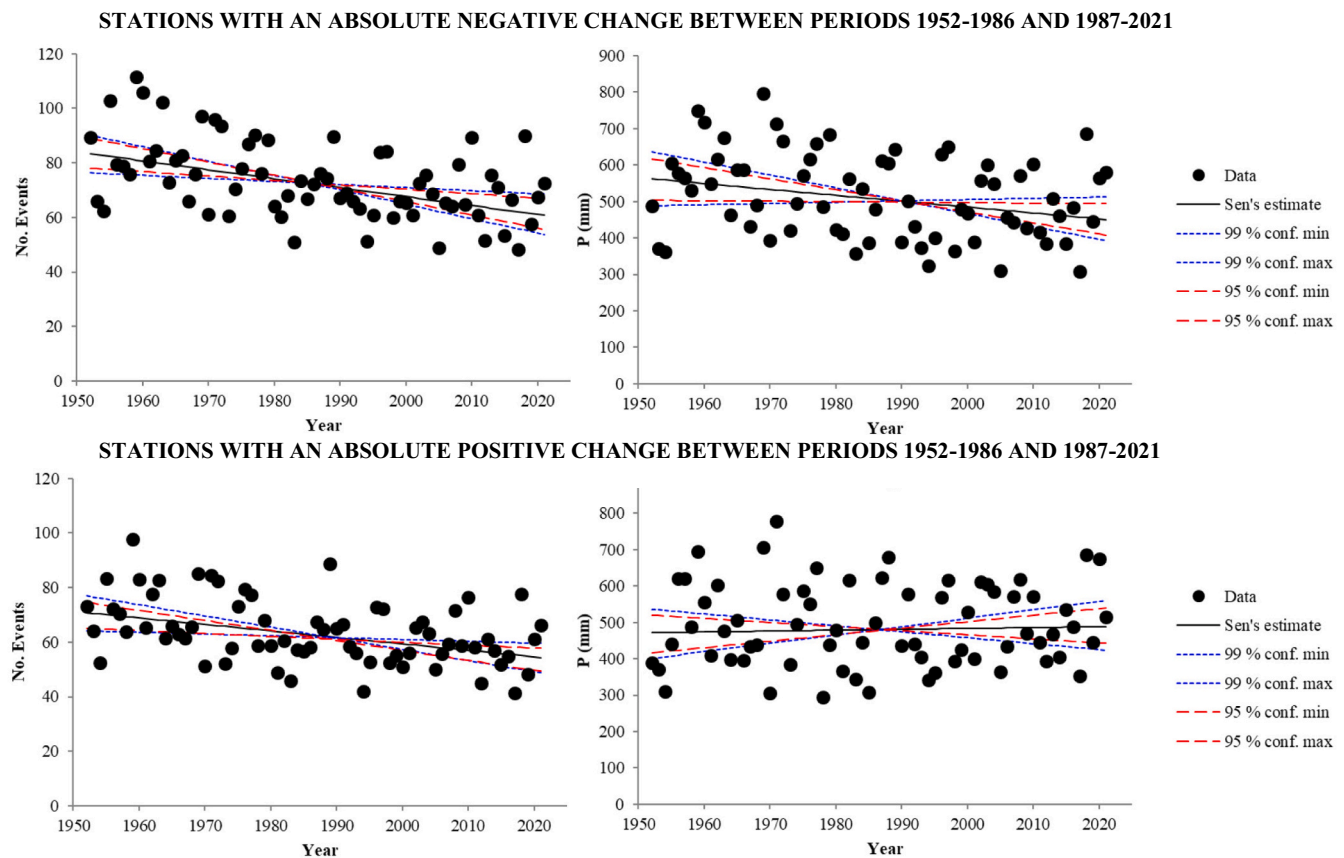


**Fig. 11.** Top images: Slopes (Sen) and confidence intervals (95–99%) for the average trend (1952–2021) in the moderate (rainfall between the 50th and 95th percentiles) daily events of all the stations that, according to Fig. 10 (top right image), show an absolute negative change between periods 1952–1986 and 1987–2021 (on the left, number of events; on the right, average rainfall accumulated per station and year for these events). Bottom images: Same analysis using all the stations that, according to Fig. 10 (top right image), show an absolute positive change between periods 1952–1986 and 1987–2021.

• Moderate rainfall, represented by the daily rainfall recorded between the 50th and 95th percentiles, is the most effective on the water balance in our study area and represents approximately 61% of total precipitation. Given its importance, any alteration to this type of rainfall may have major effects on the evolution of the water resources in the studied area and downstream areas, which are fed by the water that comes from the rivers that arise there. In fact, the impact on the economic system of the eastern coastal regions in the Iberian Peninsula (Valencian Community, Region of Murcia and eastern Andalusia) is fundamental given that the tourism and agricultural sectors are basic pillars of their economic system (Cañizares et al., 2022; Miró et al., 2021). The reduction in captured volumes is notorious throughout the study area, but is more significant in CHT, where loss is general throughout its territory, and also in CHG and CHE. In CHJ, significant losses appear in the area bordering CHT, where the Júcar, Turia and Cabriel river headwaters are located. In this declining precipitation context, studies into future climate conditions only corroborate the marked and continuing declining precipitation trend that, although already present in the short term, will become much worse in the last third of the 21st century (Miró et al., 2021). Todaro et al. (2022) support these results, especially for the medium term (2051–2070) and for the RCP4.5 emission scenario, but they differ for higher forcing (RCP8.5). It is also worth mentioning that slight increases are detected in southeastern areas (toward the Mediterranean littoral). In any case, the trend of the pluviometric stations with reductions between the 1952–1986 and 1987–2021 periods is very clearly negative for this type of rainfall, and also in terms of the number of events and precipitation volumes. In contrast, the stations with the biggest rainfall increase during the

most recent period do not show any significant positive trend over time, and events in the lower range also tend to decrease. Therefore, this type of rainfall is expected to continue to decrease in forthcoming years in the studied area and, hence, the water capacity of downstream-dependent areas will decrease. Some hydrological studies have already pointed out this trend for the Tagus basin. Thus, Mezger et al. (2022) observe a general trend toward decreased availability of water resources, which is made visible in the trend toward decreased flow, an aspect that they relate to the combination of several non climatic factors, among which the very marked role of increased irrigated land (of the order of 400%) should be highlighted. These results present a critical scenario of negative trends in river flows of several headwaters in the Iberian Peninsula at the same time, and these basins are not even anthropized (Martínez-Fernández et al., 2013). Therefore, they determine a key climatic reality to be taken into account in conjunction with other non climatic factors of the territory.

Other studies have analyzed trends in several rivers of the Iberian Peninsula and obtained similar results. Miró et al. (2018) detected a negative trend and loss of precipitation in the Júcar river headwaters. Their results support those herein obtained. Likewise, in the Ebro river headwaters located in the Pyrenees, negative trends in precipitation have been shown as one of the causes of loss of runoff from rivers (López-Moreno et al., 2008). Similarly, López-Moreno et al. (2010) have detected a general trend in decreasing precipitation, rainfall days and precipitation intensity, prolonged dry spell duration in the NE Iberian Peninsula, and conferred special relevance to the headwaters of basins in winter and spring months. In the Duero basin, less runoff from river



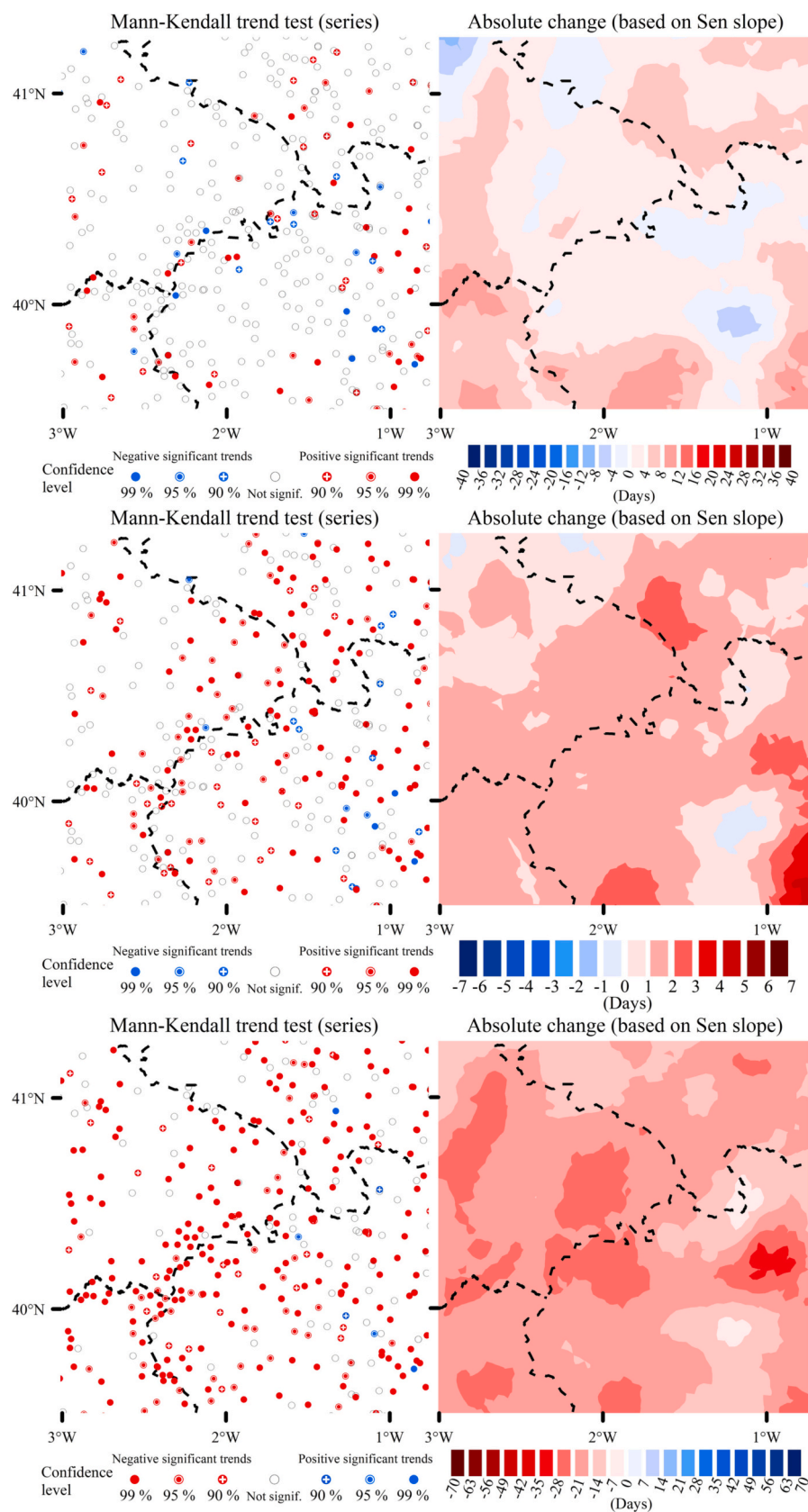


**Fig. 12.** Significant trends and absolute change in days for annual maximum dry spell duration (top images), annual average dry spell (center images) and annual average wet spell durations (bottom images) for the 1952–2021 period.

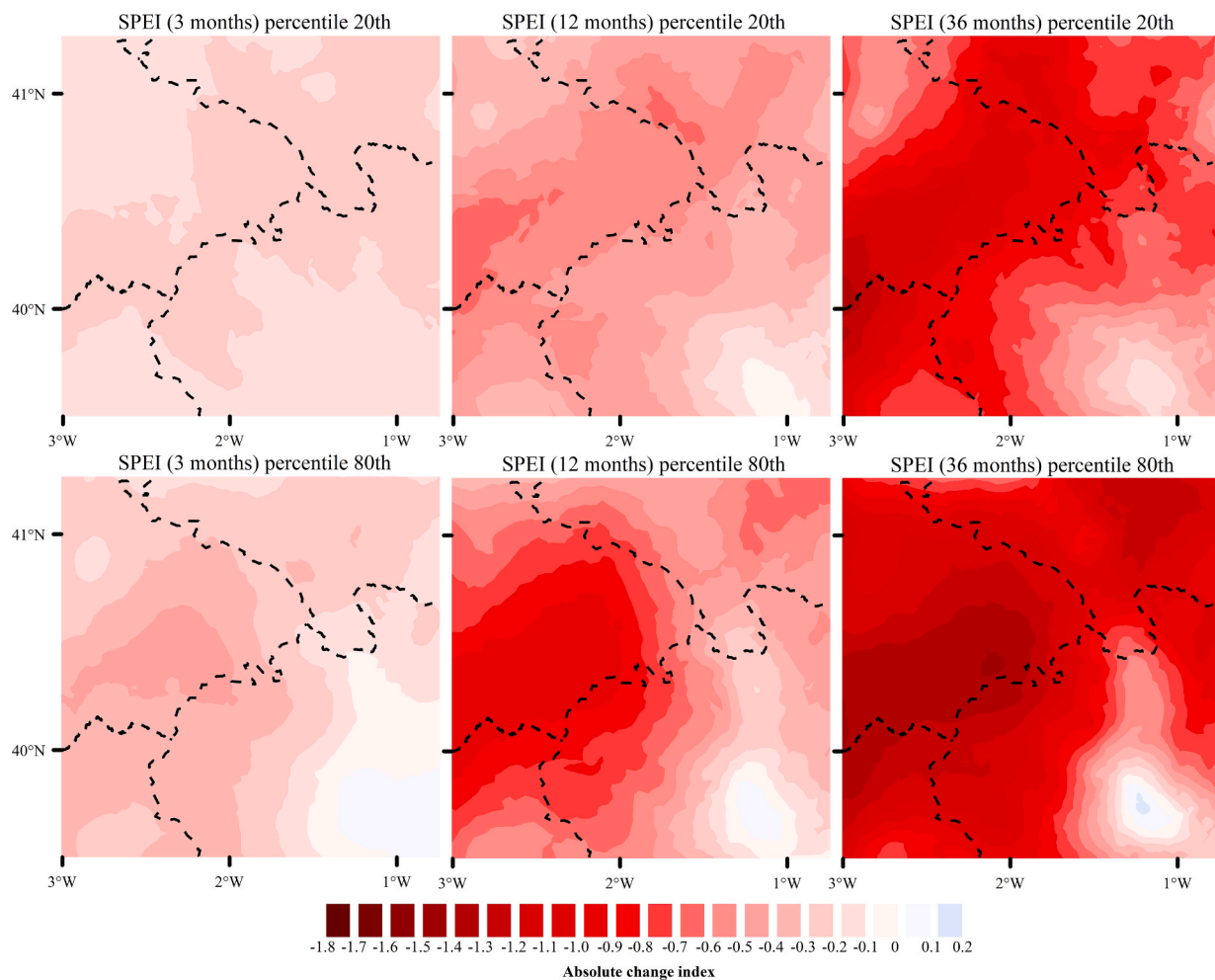


**Fig. 13.** Top: Absolute change between the 20th percentile SPEI daily values on the 3- (left), 12- (center) and 36- (right) month time scales of the two 35-year periods (1952–1986 and 1987–2021). Bottom: the same analysis for the 80th percentile SPEI daily values.

headwaters in spring due to loss of precipitation and rises in temperature has also been reported (Morán-Tejeda et al., 2010).

The drought evolution analysis reveals that the most recent period (1987–2021) is drier than the previous one (1952–1986), with lower SPEI values throughout the study area, except the southeastern end of CHJ, where slight increases are recorded. At the same time, the trend analysis reveals that most analyzed stations show negative and statistically significant trends, although the results differ according to the employed time scale. As the time scale used to carry out the study prolongs, the number of stations with a negative trend increases, and exceeds 80% in the long-term analysis (36 months). In turn, the wide interannual variability in precipitation, typical of the Mediterranean region, means that the high-frequency oscillations found in the short-term analysis (3 months) do not allow trends to be detected. However when the time scale is extended, and medium-term (12 months) and long-term (36 months) analyses are carried out, drought periods are clearly identified. This is indicative of a noticeable trend toward chronic long-term socio-economic drought conditions.

From the 1980s to the present-day, drought periods clearly predominate, many of which have lasted more than one decade. The situation of CHT is particularly complicated because, in the last 4 decades, there has hardly been any period without drought, which have generally been short (<1 year). The situation is similar in the other analyzed basins, but the duration of the periods with SPEI values above 0 has been longer. These results agree with those obtained by Lorenzo-Lacruz et al. (2010) in the Tagus river headwaters for the 1961–2006 study period.

They confirm the continuity of the severe drought period that this area is undergoing. For NE Catalonia, Serra et al. (2006) have also detected a significant increase in the duration of dry periods, which supports the results obtained for this sector of the eastern Iberian Peninsula.

The causes of these trends appear to be closely linked with changes in the general atmospheric circulation patterns on the southern edge of mid-latitudes and subtropical latitudes. The study area particularly depends on the range of the polar front associated with westerly winds of Atlantic origin (Millán et al., 1998, 2005; Miró et al., 2018). More precisely, a northward expansion of subtropical high pressures has been identified with a greater predominance of the Azores anticyclone over the Iberian Peninsula, a contraction of the circumpolar vortex to the north, plus loss of weight for Atlantic flows in the region (Cresswell-Clay et al., 2022; Frauenfeld and Davis, 2003; Grise et al., 2019; Miró et al., 2015; Trenberth et al., 2007).

## 5. Conclusions

The mountain ranges of the southern Iberian System are a particularly relevant area for the water system recharge and drought risk management of several Mediterranean basins in the Iberian Peninsula. This study reveals a critical situation for this hydrological context due to the continuous loss of precipitation over the last 35 years, and the situation will continue to worsen in forthcoming years. This leads to the fact that we find ourselves in a drought period, which is a pressing matter in the four analyzed hydrological basins. In this regard, it is

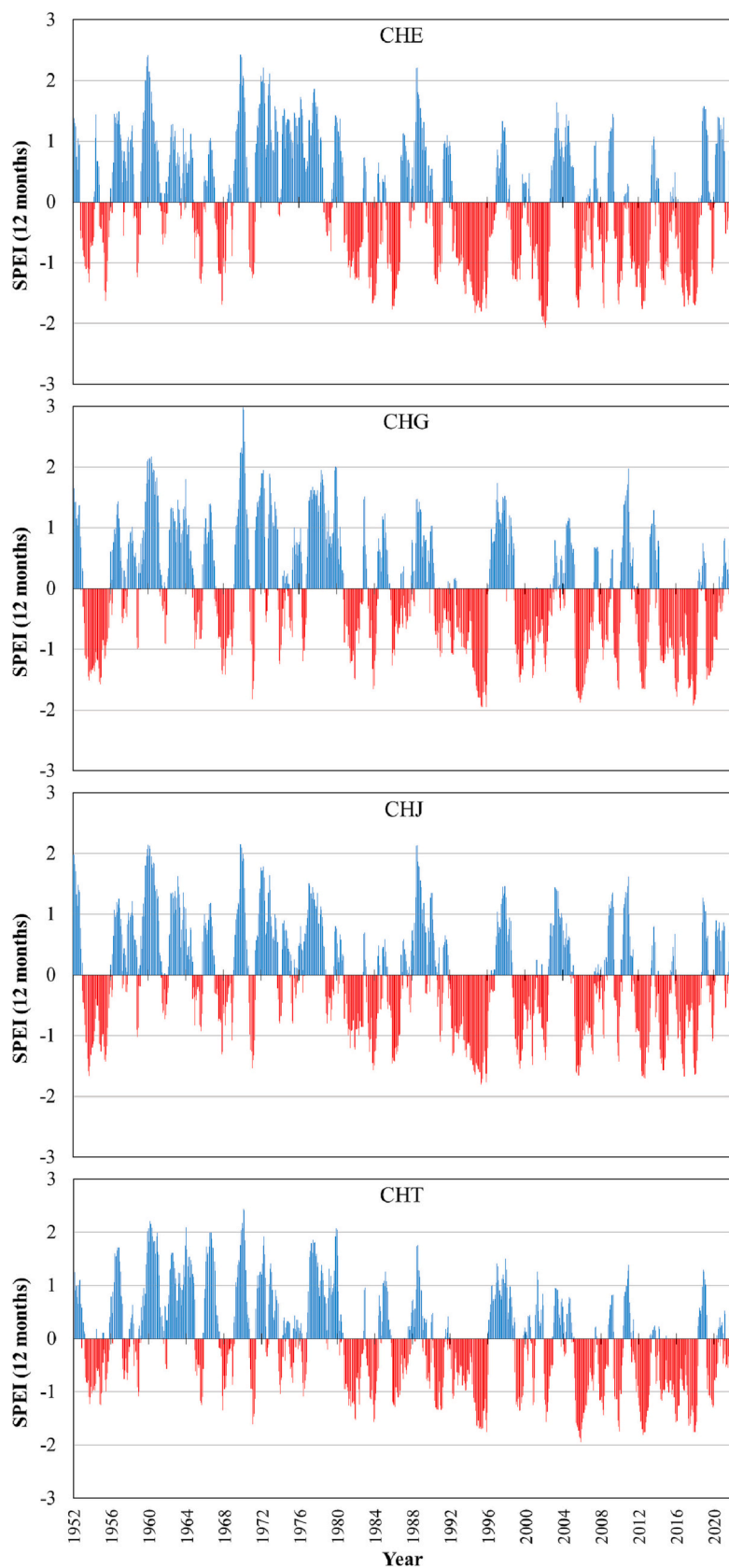


**Fig. 14.** Time series of the average daily SPEI values on the 12- and 36-month time scales for the 1952–2021 period and all the CHE, CHG, CHJ and CHT weather stations.



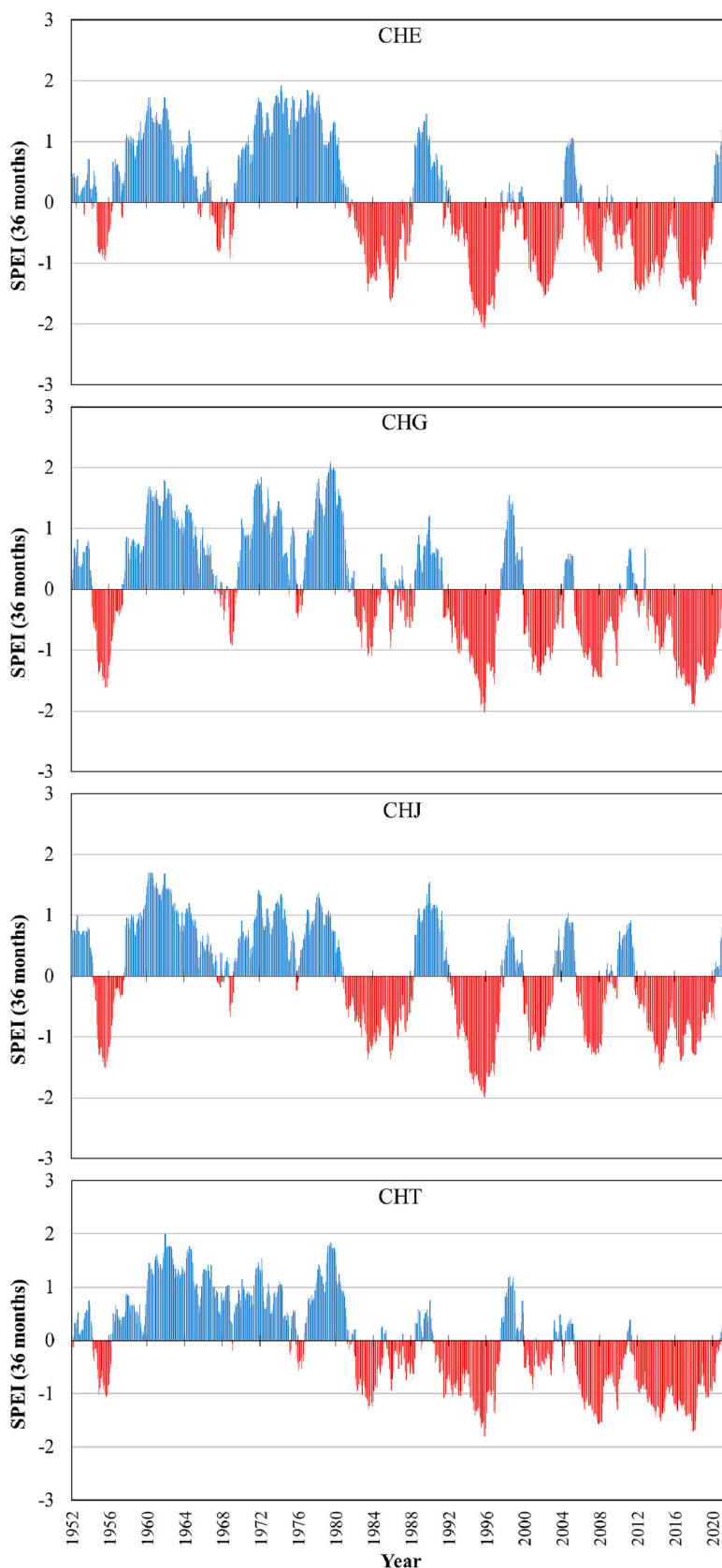


Fig. 14. (continued).

worth mentioning a remarkable trend toward chronic long-term drought conditions for the whole area and its hydrological-socio-economic connections with a large Mediterranean coastal region. The situation is

particularly alarming in the Tagus basin headwaters, a situation that dates back to the 1980s.

The water provided by these headwaters, particularly from Júcar and

Turia, as well as that of the Tagus (the last one via the artificial Tagus-Segura Water Transfer Canal), is key for urban, agricultural, industrial and tourism water supply in the administrative communities of the Valencian Community and Region of Murcia, particularly on the coastal strip, where the largest population and economic activity of these regions concentrate. Therefore, the conclusions of this study are extremely relevant for the future hydrological planning and to achieve alternatives regarding the higher risk associated with the droughts of these regions. Camarasa-Belmonte et al. (2020) have already published some studies which, bearing in mind the general decreased precipitation trend, highlight the change in the valuation of water in the eastern interior of Spain, which has gone from being a resource to being a very pronounced risk to be taken into account.

Finally, it is necessary to bear in mind the impacts on both this natural environment of high ecological value (the mountain ranges of the southern Iberian Range) and those produced beyond, such as feeding the aquifers of the La Mancha Region and of the wetlands located on the southern Iberian plateau (i.e., the Tablas de Daimiel National Park), because their environmental value is very high.

Supplementary data to this article can be found online at <https://doi.org/10.1016/j.atmosres.2023.106695>.

## Declaration of Competing Interest

The authors declare that they have no known competing financial interests or personal relationships that could have appeared to influence the work reported in this paper.

## Data availability

The authors do not have permission to share data.

## Acknowledgements

This study has been funded by the Spanish Ministry of Science and Innovation through Research Project PID2020-118797RB-I00 (MCIN/AEI/10.13039/501100011033) and by the Generalitat Valenciana with Research Project PROMETEO/2021/016 (Conselleria d'Innovació, Universitats, Ciència i Societat Digital).

## References

- Alpert, P., Bengali, T., Baharad, A., Benjamini, Y., Yekutieli, D., Colacino, M., Diodato, L., Ramis, C., Homar, V., Romero, R., Michaelides, S., Manes, A., 2002. The paradoxical increase of Mediterranean extreme daily rainfall in spite of decrease in total values. *Geophys. Res. Lett.* 29 (11) <https://doi.org/10.1029/2001GL013554>.
- Barcikowska, M.J., Kapnick, S., Feser, F., 2018. Impact of large-scale circulation changes in the North Atlantic sector on the current and future Mediterranean winter hydroclimate. *Clim. Dyn.* 50, 2039–2059. <https://doi.org/10.1007/s00382-017-3735-5>.
- Beguieria, S., Vicente-Serrano, S.M., Reig, F., Latorre, B., 2013. Standardized precipitation evapotranspiration index (SPEI) revisited: parameter fitting, evapotranspiration models, tools, datasets and drought monitoring. *Int. J. Climatol.* 34, 3001–3023. <https://doi.org/10.1002/joc.3887>.
- Bladé, I., Castro Díez, Y., 2010. Atmospheric trends in the Iberian Peninsula during the instrumental period in the context of natural variability. In: Pérez, F.F., Boscolo, R. (Eds.), *Clima en España: pasado, presente y futuro*, pp. 25–42.
- Camarasa-Belmonte, A., Rubio, M., Salas, J., 2020. Rainfall events and climate change in Mediterranean environments: an alarming shift from resource to risk in Eastern Spain. *Nat. Hazards* 103, 423–445. <https://doi.org/10.1007/s11069-020-03994-x>.
- Cañizares, A.O., Cantos, J.O., Baños Castañeira, C.J., 2022. The Effects of Climate Change on the Tagus-Segura Transfer: Diagnosis of the Water Balance in the Vega Baja del Segura (Alicante, Spain). *Water* 14, 2023. <https://doi.org/10.3390/w14132023>.
- Castro, M.D., Martín-Vide, J., Alonso, S., 2005. El clima de España: Pasado, presente y escenarios de clima para el siglo XXI. In: Moreno Rodríguez, J.M. (Ed.), *Evaluación Preliminar de los Impactos en España Por Efecto del Cambio Climático*. Ministerio de Medio Ambiente y Universidad de Castilla-La Mancha, pp. 1–64.
- Christensen, J.H., Hewitson, A., Busiuc, A., Chen, X., Gao, I., Held, R., Jones, R.K., Kolli, W.T., Kwon, R., Laprise, V., Magaña Rueda, L., Mearns, C.G., Menéndez, J., Räisänen, A., Rinke, A., Sarr, A., Whetton, P., 2007. Regional climate projections. In: Solomon, S., Qin, D., Manning, M., Chen, Z., Marquis, M., Averyt, K.B., Tignor, M., Miller, H.L. (Eds.), *Climate Change 2007: The Physical Science Basis, Contribution of Working Group I to the Fourth Assessment Report of the Intergovernmental Panel on Climate Change*. Cambridge University Press, Cambridge, New York.
- Clemente, M.A., et al., 2018. Spatio-temporal analysis of drought in peninsular Spain. Influence of the main teleconnection patterns. In: Montávez, J.P., et al. (Eds.), *Climate: Air, Water, Land and Fire*, pp. 569–579.
- Cos, J., Doblas-Reyes, F., Jury, M., Marcos, R., Bretonnière, P.A., Samsó, M., 2022. The Mediterranean climate change hotspot in the CMIP5 and CMIP6 projections. *Earth Syst. Dynam.* 13, 321–340. <https://doi.org/10.5194/esd-13-321-2022>.
- Cresswell-Clay, N., Ummenhofer, C.C., Thatcher, D.L., Wanamaker, A.D., Denniston, R. D., Asmerom, Y., Polyak, V.J., 2022. Twentieth-century Azores High expansion unprecedented in the past 1,200 years. *Nat. Geosci.* 15, 548–553. <https://doi.org/10.1038/s41561-022-00971-w>.
- De Luis, M., González-Hidalgo, J.C., Longares, L.A., Stepánek, P., 2009. Seasonal precipitation trends in the Mediterranean Iberian Peninsula in second half of 20th century. *Int. J. Climatol.* 29, 1312–1323. <https://doi.org/10.1002/joc.1778>.
- De Luis, M., González-Hidalgo, J.C., Brunetti, M., Longares, L.A., 2011. Precipitation concentration changes in Spain 1946–2005. *Nat. Hazards Earth Syst. Sci.* 11, 1259–1265. <https://doi.org/10.5194/nhess-11-1259-2011>.
- Domonkos, P., 2014. The ACMANT2 software package. In: Eighth Seminar for Homogenization and Quality Control in Climatological Databases and Third Conference on Spatial Interpolation Techniques in Climatology and Meteorology, WMO WCDMP-84. World Meteorological Organization (WMO), Geneva, pp. 46–72.
- Domonkos, P., 2015. Homogenization of precipitation time series with ACMANT. *Theor. Appl. Climatol.* 122, 303–314. <https://doi.org/10.1007/s00704-014-1298-5>.
- Frauenfeld, O.W., Davis, R.E., 2003. Northern Hemisphere circumpolar vortex trends and climate change implications. *J. Geophys. Res. Atmos.* 108, 4423. <https://doi.org/10.1029/2002JD002958>.
- Gallart, F., Llorens, P., 2004. Observations on land cover changes and water resources in the headwaters of the Ebro catchment, Iberian Peninsula. *Phys. Chem. Earth Parts A/B/C* 29 (11–12), 769–773. <https://doi.org/10.1016/j.pce.2004.05.004>.
- García-Herrera, R., Hernández, E., Barriopedro, D., Paredes, D., Trigo, R.M., Trigo, I., Mendes, M.A., 2007. The outstanding 2004/05 Drought in the Iberian Peninsula: Associated Atmospheric Circulation. *J. Hydrometeorol.* 8, 483–498. <https://doi.org/10.1175/JHM578.1>.
- Gil Olcina, A., 1995. Conflictos autonómicos sobre trasvases de agua en España. *Investig. Geográf.* 13, 17–28. <https://doi.org/10.14198/INGEO1995.13.05>.
- Giorgi, F., 2006. Climate change hot-spots. *Geophys. Res. Lett.* 33 (8), L08707. <https://doi.org/10.1029/2006GL025734>.
- Goodess, C.M., Jones, P.D., 2002. Links between circulation and changes in the characteristics of Iberian rainfall. *Int. J. Climatol.* 22, 1593–1615. <https://doi.org/10.1002/joc.810>.
- Grise, K.M., Davis, S.M., Simpson, I.R., Waugh, D.W., Fu, Q., Allen, R.J., Rosenlof, K.H., Ummenhofer, C.C., Karneuskas, K.B., Maycock, A.C., Quan, X., Birner, T., Staten, P. W., 2019. Recent tropical expansion: natural variability or forced response? *J. Clim.* 32, 1551–1571. <https://doi.org/10.1175/JCLI-D-18-0444.1>.
- Gualdi, S., Somot, S., May, W., Castellari, S., Déqué, M., Adani, M., Artale, V., Bellucci, A., Breitgand, J.S., Carillo, A., Cornes, R., Dell'Aquila, A., Dubois, C., Efthymiadis, D., Elizalde, A., Gimeno, L., Goodess, C.M., Harzallah, A., Krichak, S.O., Kuglitsch, F.G., Leckebusch, G.C., L'Hévéder, B., Li, L., Lionello, P., Luterbacher, J., Mariotti, A., Navarra, A., Nieto, R., Nissen, K.M., Oddo, P., Ruti, P., Sanna, A., Sannino, G., Scoccimarro, E., Sevaut, F., Struglia, M.V., Toreti, A., Ulbrich, U., Xoplaki, E., 2013. Future climate projections. In: Navarra, A., Tubiana, L. (Eds.), *Regional Assessment of Climate Change in the Mediterranean*. Springer, Dordrecht, pp. 53–118. [https://doi.org/10.1007/978-94-007-5781-3\\_3](https://doi.org/10.1007/978-94-007-5781-3_3).
- Held, I.M., Soden, B.J., 2006. Robust responses of the hydrological cycle to global warming. *J. Clim.* 19, 5686–5699. <https://doi.org/10.1175/JCLI3990.1>.
- Ilin, A., Raiko, T., 2010. Practical approaches to principal component analysis in the presence of missing values. *J. Mach. Learn. Res.* 11, 1957–2000. <https://dl.acm.org/doi/10.5555/1756006.1859917>.
- Intergovernmental Panel on Climate Change (IPCC), 2022. *Climate Change 2022: Impacts, Adaptation, and Vulnerability*. In: Pörtner, H.-O., Roberts, D.C., Tignor, M., Poloczanska, E.S., Mintenbeck, K., Alegria, A., Craig, M., Langsdorf, S., Lösschke, S., Möller, V., Okem, A., Rama, B. (Eds.), *Contribution of Working Group II to the Sixth Assessment Report of the Intergovernmental Panel on Climate Change*. Cambridge University Press, In Press.
- Kendall, M.G., 1962. *Rank Correlation Methods*. Charles Griffin Book Series, London.
- Kundzewicz, Z.W., Mata, L.J., Arnell, N.W., Döll, P., Kabat, P., Jiménez, B., Miller, K.A., Oki, T., Sen, Z., Shiklomanov, I.A., 2007. Freshwater resources and their management. In: Parry, M.L., Canziani, O.F., Palutikof, J.P., van der Linden, P.J., Hanson, C.E. (Eds.), *Climate Change 2007 Impacts, Adaptation and Vulnerability. Contribution of Working Group II to the Fourth Assessment Report of the Intergovernmental Panel on Climate Change*. Cambridge University Press, Cambridge, UK, pp. 173–210.
- Lana, X., Serra, C., Burguño, A., 2001. Patterns of monthly rainfall shortage and excess in terms of the standardized precipitation index for Catalonia (NE Spain). *Int. J. Climatol.* 21, 1669–1691. <https://doi.org/10.1002/joc.697>.
- Lana, X., Martínez, M.D., Burguño, A., Serra, C., Martín-Vide, J., Gómez, L., 2006. Distributions of long dry spells in the Iberian Peninsula, years 1951–1990. *Int. J. Climatol.* 26, 1999–2021. <https://doi.org/10.1002/joc.1354>.
- Lionello, P., Scarascia, L., 2018. The relation between climate change in the Mediterranean region and global warming. *Reg. Environ. Chang.* 18, 1481–1493. <https://doi.org/10.1007/s10113-018-1290-1>.
- Lionello, P., Abrantes, F., Congedi, L., Dulac, R., Gacic, M., Gomis, D., Goodess, C., Hoff, H., Kutiel, H., Luterbacher, J., Planton, S., Reale, M., Schröder, K., Struglia, M. V., Toreti, A., Tsimplis, M., Ulbrich, U., Xoplaki, E., 2012. Introduction: Mediterranean climate: background information. In: Lionello, P. (Ed.), *The Climate*

- of the Mediterranean Region. From the Past to the Future. Elsevier (Netherlands), Amsterdam. <https://doi.org/10.1016/B978-0-12-416042-2.00012-4> xxxv-xxxx, ISBN: 9780124160422.
- López-Moreno, J.I., Beguería, S., García-Ruiz, J.M., 2004. The management of a large Mediterranean reservoir: Storage regimes of the Yesa reservoir, Upper Aragon River Basin, Central Spanish Pyrenees. *Environ. Manag.* 34, 508–515. <https://doi.org/10.1007/s00267-003-0249-1>.
- López-Moreno, J.I., Beniston, M., García-Ruiz, J.M., 2008. Environmental change and water management in the Pyrenees facts and future perspectives for Mediterranean mountains. *Glob. Planet. Chang.* 61, 300–312. <https://doi.org/10.1016/j.gloplacha.2007.10.004>.
- López-Moreno, J.I., Vicente-Serrano, S.M., Gimeno, L., Nieto, R., 2009. Stability of the seasonal distribution of precipitation in the headwaters of the Tagus River: Observations since 1950 and projections for the 21st century. *Geophys. Res. Lett.* 36, L10703. <https://doi.org/10.1029/2009GL037956>.
- López-Moreno, J.I., Vicente-Serrano, S.M., Angulo-Martínez, M., Beguería, S., Kenawy, A., 2010. Trends in daily precipitation on the northeastern Iberian Peninsula, 1955–2006. *Int. J. Climatol.* 30, 1026–1041. <https://doi.org/10.1002/joc.1945>.
- Lorenzo-Lacruz, J., Vicente-Serrano, S.M., López-Moreno, J.I., Beguería, S., García-Ruiz, J.M., Cuadrat, J., 2010. The impact of droughts and water management on various hydrological systems in the headwaters of the Tagus River (Central Spain). *J. Hydrol.* 386, 13–26. <https://doi.org/10.1016/j.jhydrol.2010.01.001>.
- Mann, H.B., 1945. Nonparametric test against trend. *Econometrica* 13 (3), 245–259. <https://doi.org/10.2307/1907187>.
- Martínez-Fernández, J., Sánchez, N., Herrero-Jiménez, C.M., 2013. Recent trends in rivers with near-natural flow regime: the case of the river headwaters in Spain. *Prog. Phys. Geogr.* 37 (5), 685–700. <https://doi.org/10.1177/0309133313496834>.
- Martín-Vide, J., Olcina-Cantos, J., 2001. *Climas y tiempos de España*. Alianza Editorial, Madrid.
- Melgarejo Moreno, J., López Órtiz, M.I., 2020. External: The socio-economic value of the Tagus-Segura aqueduct for the province of Alicante. In: Melgarejo Moreno, J., Fernández Mejuto, M. (Eds.), *Water in the province of Alicante*. Diputación Provincial de Alicante and University of Alicante, pp. 157–182.
- Mezger, G., De Stefano, L., González del Tánago, M., 2022. Analysis of the Evolution of Climatic and Hydrological Variables in the Tagus River Basin, Spain. *Water* 14, 818. <https://doi.org/10.3390/w14050818>.
- Millán, M.M., Estrela, M.J., Vallejo, R., 1998. Evaluation of the hydrological inputs in the Mediterranean basin. In: *Proceedings of the First Int. Conf. on Fog and Fog Collection*. Vancouver, Canada, pp. 281–284.
- Millán, M.M., Estrela, M.J., Miró, J.J., 2005. Rainfall Components: Variability and Spatial distribution in a Mediterranean Area (Valencia Region). *J. Clim.* 18, 2682–2705. <https://doi.org/10.1175/JCLI3426.1>.
- Miró, J.J., Estrela, M.J., Pastor, F., Millán, M., 2009. Comparative analysis of trends in precipitation, by different inputs, between the hydrological domains of the Segura and Júcar rivers (1958–2008). *Investig. Geográf.* 49, 129–157. <https://doi.org/10.14198/INGEO2009.49.07>.
- Miró, J.J., Estrela, M.J., Olcina-Cantos, J., 2015. Statistical downscaling and attribution of air temperature change patterns in the Valencia region (1948–2011). *Atmos. Res.* 156, 189–212. <https://doi.org/10.1016/j.atmosres.2015.01.003>.
- Miró, J.J., Caselles, V., Estrela, M.J., 2017. Multiple imputation of rainfall missing data in the Iberian Mediterranean context. *Atmos. Res.* 197, 313–330. <https://doi.org/10.1016/j.atmosres.2017.07.016>.
- Miró, J.J., Estrela, M.J., Caselles, V., Gómez, I., 2018. Spatial and temporal rainfall changes in the Júcar and Segura basins (1955–2016): Fine-scale trends. *Int. J. Climatol.* 38, 4699–4722. <https://doi.org/10.1002/joc.5689>.
- Miró, J.J., Estrela, M.J., Olcina-Cantos, J., Martín-Vide, J., 2021. Future Projection of Precipitation changes in the Júcar and Segura River Basins (Iberian Peninsula) by CMIP5 GCMs Local Downscaling. *Atmosphere* 12, 879. <https://doi.org/10.3390/atmos12070879>.
- Morales Gil, A., Rico Amorós, A.M., Hernández, M., 2005. *El trasvase Tagus-Segura*. Observatorio Medioambiental, 8, 73–110.
- Morán-Tejeda, E., Ceballos-Barbancho, A., Llorente-Pinto, J.M., 2010. Hydrological response of Mediterranean headwaters to climate oscillations and land-cover changes: the mountains of Duero River basin (Central Spain). *Glob. Planet. Chang.* 72 (1–2), 39–49. <https://doi.org/10.1016/j.gloplacha.2010.03.003>.
- Peña-Gallardo, M., Gámiz-Fortis, S., Castro-Díez, Y., Esteban-Parra, M.J., 2016. Comparative analysis of drought indices in Andalusia for the period 1901–2012. *Cuadernos de Investig. Geográf.* 42 (1), 67–88. <https://doi.org/10.18172/cig.2946>.
- Piervitali, E., Colacino, M., Conte, M., 1998. Rainfall over the Central-Western Mediterranean Basin in the period 1951–1995, part I: Precipitation Trends. *Nuovo Cimento* 21, 331–344.
- Randall, D.A., Wood, R.A., Bony, S., Colman, R., Fichetef, T., Fyfe, J., Kattsov, V., Pitman, A., Shukla, J., Srinivasan, J., Stouffer, R.J., Sumi, A., Taylor, K.E., 2007. *Climate models and their evaluation*. In: Solomon, S., Quin, D., Manning, M., Chen, Z., Marquis, M., Averyt, K.B., Tignor, M., Miller, H.L. (Eds.), *Climate Change 2007: The Physical Science Basis, Contribution of Working Group I to the Fourth Assessment Report of the Intergovernmental Panel on Climate Change*. Cambridge University Press, Cambridge, New York.
- Serra, C., Burgueño, A., Martínez, M.D., Lana, X., 2006. Trends in dry spells across Catalonia (NE Spain) during the second half of the 20th century. *Histor. Appl. Climatol.* 85, 165–183. <https://doi.org/10.1007/s00704-005-0184-6>.
- Serrano, A., Mateos, V.L., García, J.A., 1999. Trend analysis of monthly precipitation over the Iberian Peninsula for the period 1921–1995. *Phys. Chem. Earth, Part B: Hydrol., Oceans and Atmosphere* 24 (1–2), 85–90. [https://doi.org/10.1016/S1464-1909\(98\)00016-1](https://doi.org/10.1016/S1464-1909(98)00016-1).
- Stage, J.H., Tallaksen, L.M., Gudmundsson, L., Van Loon, A.F., Stahl, K., 2015. Candidate distributions for climatological drought indices (SPI and SPEI). *Int. J. Climatol.* 35 (13), 4027–4040. <https://doi.org/10.1002/joc.4267>.
- Stage, J.H., Kingston, D.G., Tallaksen, L.M., Hannah, D.M., 2017. Observed drought indices show increasing divergence across Europe. *Sci. Rep.* 7, 14045. <https://doi.org/10.1038/s41598-017-14283-2>.
- State Meteorological Agency (AEMET), 2018. *Climate Maps of Spain (1981–2010) and ETo (1996–2016)*. Ministerio para la Transición Ecológica and Agencia Estatal de Meteorología, Madrid. <https://doi.org/10.31978/014-18-004-2>.
- Tanguy, M., Prudhomme, C., Smith, K., Hannaford, J., 2017. Historic Gridded potential Evapotranspiration (PET) Based on Temperature-Based McGuinness-Bordne Equation Calibrated for the UK (1891–2015). NERC Environmental Information Data Centre. <https://doi.org/10.5285/17b9c4f7-1c30-4b6f-b2fe-f7780159939c>.
- Thornes, J.B., López-Bermúdez, F., Woodward, J.C., 2009. Hydrology, river regimes, and sediment yield. In: Woodward, J.C. (Ed.), *The Physical Geography of the Mediterranean*. Oxford University Press, Oxford, pp. 229–253.
- Todaro, V., D'Oria, M., Secchi, D., Zanini, A., Tanda, M.G., 2022. Climate Change over the Mediterranean Region: Local Temperature and Precipitation Variations at five pilot Sites. *Water* 14, 2499. <https://doi.org/10.3390/w14162499>.
- Trenberth, K.E., Jones, P.D., Ambenje, P., Bojariu, R., Easterling, D., Klein Tank, A., Parker, D., Rahimzadeh, F., Renwick, J.A., Rusticucci, M., Soden, B., Zhai, P., 2007. Observations: Surface and Atmospheric Climate Change. Available online: <https://www.ipcc.ch/site/assets/uploads/2018/02/ar4-wg1-chapter3-1.pdf>. accessed on 22 September 2022.
- Ulbrich, U., Xoplaki, E., Dobricic, S., García-Herrera, R., Lionello, P., Adani, M., Baldi, M., Barriopedro, D., Coccimiglio, P., Dalu, G., Efthymiadis, D., Gaetani, M., Galati, M.B., Gimeno, L., Goodess, C.M., Jones, P.D., Kuglitsch, F.G., Leckebusch, G.C., Luterbacher, J., Marcos-Moreno, M., Mariotti, A., Nieto, R., Nissen, K.M., Pettenuzzo, D., Pinardi, N., Pino, C., Shaw, A.G.P., Sousa, P., Toreti, A., Trigo, R.M., Tsimplis, M., 2013. Past and current climate changes in the Mediterranean region. In: Navarra, A., Tubiana, L. (Eds.), *Regional Assessment of Climate Change in the Mediterranean*. Springer, Dordrecht, pp. 9–52. [https://doi.org/10.1007/978-94-007-5781-3\\_2](https://doi.org/10.1007/978-94-007-5781-3_2).
- Vicente-Serrano, S.M., 2006. Spatial and temporal analysis of droughts in the Iberian Peninsula (1910–2000). *Hydrol. Sci. J.* 51 (1), 83–97. <https://doi.org/10.1623/hysj.51.1.83>.
- Vicente-Serrano, S.M., González-Hidalgo, J.C., De Luis, M., Raventós, J., 2004. Drought patterns in the Mediterranean area: the Valencia region (eastern Spain). *Clim. Res.* 26, 5–15. <https://doi.org/10.3354/cr026005>.
- Vicente-Serrano, S.M., Beguería, S., López-Moreno, J.I., 2010. A Multiscalar Drought Index Sensitive to Global Warming: the standardized Precipitation Evapotranspiration Index. *J. Clim.* 23 (7), 1696–1718. <https://doi.org/10.1175/2009JCLI2909.1>.
- Vicente-Serrano, S.M., Tomás-Burguera, M., Beguería, S., Reig, F., Latorre, B., Peña-Gallardo, M., Luna, M.Y., Morata, A., González-Hidalgo, J.C., 2017. A high resolution dataset of drought indices for Spain. *Data* 2 (3), 22. <https://doi.org/10.3390/data2030022>.
- Wang, S., Huang, G.H., Lin, Q.G., Li, Z., Zhang, H., Fan, Y.R., 2014. Comparison of interpolation methods for estimating spatial distribution of precipitation in Ontario, Canada. *Int. J. Climatol.* 34, 3745–3751. <https://doi.org/10.1002/joc.3941>.
- Wang, Q., Zeng, J., Qi, J., Zhang, X., Zeng, Y., Shui, W., Xu, Z., Zhang, R., Wu, X., Cong, J., 2021. A multi-scale daily SPEI dataset for drought characterization at observation stations over mainland China from 1961 to 2018. *Earth Syst. Sci. Data* 13, 331–341. <https://doi.org/10.5194/essd-13-331-2021>.
- World Meteorological Organization, 2016. Guidelines on the Definition and Monitoring of Extreme Weather and Climate Events. Available at: [https://www.wmo.int/page\\_s/prog/wcp/ccl/opace/opace2/documents/DraftversionoftheGuidelinesontheDefinitionandMonitoringofExtremeWeatherandClimateEvents.pdf](https://www.wmo.int/page_s/prog/wcp/ccl/opace/opace2/documents/DraftversionoftheGuidelinesontheDefinitionandMonitoringofExtremeWeatherandClimateEvents.pdf).
- Zappa, G., 2019. Regional Climate Impacts of Future Changes in the Mid-Latitude Atmospheric Circulation: a Storyline View. *Curr. Clim. Chang. Rep.* 5, 358–371. <https://doi.org/10.1007/s40641-019-00146-7>.